Department of Biotechnology and Chemical Technology

Effect of lignin structure on enzymatic hydrolysis of plant residues

Mika Sipponen

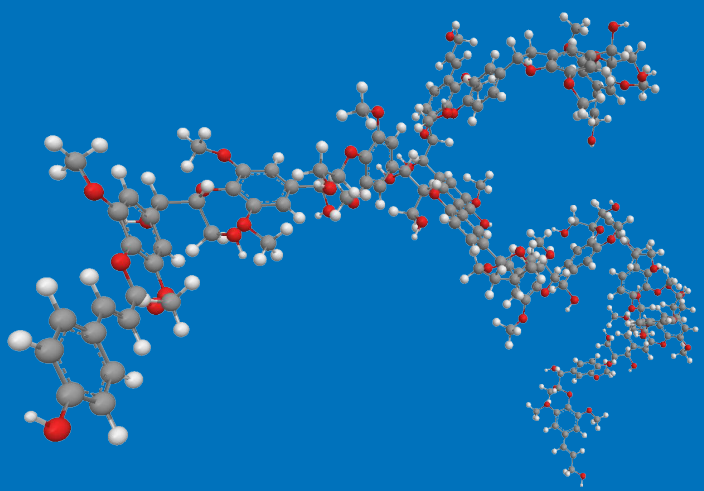

Aalto University

DOCTORAL DISSERTATIONS

Aalto University publication series
DOCTORAL DISSERTATIONS 79/2015

Effect of lignin structure on enzymatic hydrolysis of plant residues

Mika Sipponen

A doctoral dissertation completed for the degree of Doctor of Science (Technology) to be defended, with the permission of the Aalto University School of Chemical Technology, at a public examination held at the lecture hall KE2 of the school on 17 June 2015 at 12 noon.

Aalto University
School of Chemical Technology
Department of Biotechnology and Chemical Technology
Biochemistry Research Group

Supervising professor
Professor Simo Laakso

Thesis advisors
Professor Stéphanie Baumberger, AgroParisTech, France
Ph.D. Ossi Pastinen, Aalto University, Finland

Preliminary examiners
Docent Mats Galbe, Lund University, Sweden
Professor Raimo Alén, University of Jyväskylä, Finland

Opponent
Professor Claudia Crestini, Università di Roma Tor Vergata, Italy

Aalto University publication series
DOCTORAL DISSERTATIONS 79/2015

ISBN 978-952-60-6234-1 (printed)
ISBN 978-952-60-6235-8 (pdf)
ISSN-L 1799-4934
ISSN 1799-4934 (printed)
ISSN 1799-4942 (pdf)
http://urn.fi/URN:ISBN:978-952-60-6235-8

Unigrafia Oy
Helsinki 2015

Finland

441 697
Printed matter

Aalto University

Abstract

Aalto University, P.O. Box 11000, FI-00076 Aalto www.aalto.fi

Author
Mika Sipponen

Name of the doctoral dissertation
Effect of lignin structure on enzymatic hydrolysis of plant residues

Publisher School of Chemical Technology

Unit Department of Biotechnology and Chemical Technology

Series Aalto University publication series DOCTORAL DISSERTATIONS 79/2015

Field of research Applied Biochemistry

Manuscript submitted 27 February 2015 **Date of the defence** 17 June 2015

Permission to publish granted (date) 20 May 2015 **Language** English

☐ **Monograph** ☒ **Article dissertation (summary + original articles)**

Abstract

Biochemical conversion of lignocellulose into high value and energy-intensive products necessitates pretreatments that enhance enzymatic hydrolysis of lignocellulosic carbohydrates. This thesis investigated structural changes in lignin during various analytical and industrially relevant treatments of crop residues. The objective was to elucidate the effect of lignin structure on enzymatic digestibility of cellulose.

Fractionation of lignin during sequential alkaline treatments of maize stem was studied using thioacidolysis. The developed fractionation procedure enabled isolation of two structurally distinct lignin-carbohydrate fractions which comprised approximately half of the total lignin. Based on these results, the distribution of lignin structural units within the plant cell walls was identified. The effect of ball milling treatment of maize stem on lignin structure and on enzymatic carbohydrate conversion was assessed. Aryl ether linkages of lignin were not cleaved by the milling which decreased crystallinity and led to high enzymatic digestibility of cellulose. Despite the long duration of the milling only minor hydrolysis of arabinoxylan occurred. This resistance was interpreted to result from interlinkages between lignin and arabinoxylan, as revealed using the isolated lignin-carbohydrate fractions as reference materials.

A spectrophotometric method was developed for determination of lignin surface area in solid-state. The method was based on quantitative determination of binding of a cationic dye to acidic hydroxyl groups of lignin in neutral aqueous suspension. About one half of the total acidic hydroxyl groups of wheat straw alkali lignin was accessible to the dye, a phenomenon interpreted as a reflection of the three-dimensional structure of lignin.

The effect of increasing autohydrolysis severity on structure of wheat straw lignin was determined. Chemical and chromatographic analyses confirmed that lignin was cleaved during both autohydrolysis and the subsequent high intensity extraction. It was observed that lignin surface area decreased as a function of autohydrolysis severity. An underlying mechanism was proposed to include acid-catalysed hydrolysis of lignin-carbohydrate network which caused densification of lignin. One of the main results of the thesis was the inverse correlation found between lignin surface area and enzymatic digestibility of cellulose. Utilisation of this new information should lead to setting reduction of lignin surface area as an objective of lignocellulose pretreatment processes.

Keywords Lignin, structure, lignocellulose, cellulose, enzymatic hydrolysis

ISBN (printed) 978-952-60-6234-1 **ISBN (pdf)** 978-952-60-6235-8

ISSN-L 1799-4934 **ISSN (printed)** 1799-4934 **ISSN (pdf)** 1799-4942

Location of publisher Helsinki **Location of printing** Helsinki **Year** 2015

Pages 128 **urn** http://urn.fi/URN:ISBN:978-952-60-6235-8

A! Aalto-yliopisto

Tiivistelmä

Aalto-yliopisto, PL 11000, 00076 Aalto www.aalto.fi

Tekijä
Mika Sipponen

Väitöskirjan nimi
Effect of lignin structure on enzymatic hydrolysis of plant residues

Julkaisija Kemian tekniikan korkeakoulu

Yksikkö Biotekniikan ja kemian tekniikan laitos

Sarja Aalto University publication series DOCTORAL DISSERTATIONS 79/2015

Tutkimusala Soveltava biokemia

Käsikirjoituksen pvm 27.02.2015 **Väitöspäivä** 17.06.2015

Julkaisuluvan myöntämispäivä 20.05.2015 **Kieli** Englanti

☐ **Monografia** ☒ **Yhdistelmäväitöskirja (yhteenveto-osa + erillisartikkelit)**

Tiivistelmä

Lignoselluloosan biokemiallinen muuntaminen korkeamman jalostusarvon ja energiatiheyden yhdisteiksi edellyttää esikäsittelyjä, joilla tehostetaan lignoselluloosan hiilihydraattien entsymaattista hydrolyysiä. Väitöskirjassa tutkittiin viljelykasvien korjuutähteiden sisältämän ligniinin muutoksia analyyttisten ja teollisesti merkittävien käsittelyjen vaikutuksesta. Päämääränä oli selvittää ligniinin rakenteen vaikutus selluloosan entsymaattiseen hydrolysoitumiseen.

Ligniinin fraktioituminen maissin korren perättäisissä alkalisissa käsittelyissä tutkittiin tioasidolyysillä. Kehitetyllä fraktiointimenetelmällä saatiin erotettua kaksi rakenteeltaan poikkeavaa ligniini-hiilihydraattijaetta, jotka yhdessä vastasivat noin puolta ligniinin kokonaismäärästä. Tulosten perusteella identifioitiin ligniinin rakenneyksiköiden jakautuminen kasvisolukossa. Kuulamyllyjauhatuksella suoritetulla käsittelyllä selvitettiin vaikutukset maissin korren ligniinin rakenteeseen ja hiilihydraattien entsymaattiseen hydrolyysiin. Ilmeni, että ligniinin aryylieetterisidokset eivät pilkkoutuneet jauhatuksessa, joka vähensi selluloosan kiteisyyttä ja kohotti entsymaattista hydrolyysiastetta. Pitkäkestoisesta jauhatuksesta huolimatta arabinoksylaani hydrolysoitui heikosti. Ligniini-hiilihydraattijakeita vertailuaineena käyttäen ilmiön tulkittiin johtuvan arabinoksylaanin ja ligniinin ristisidoksista.

Kiinteässä olomuodossa olevan ligniinin pinta-alan määrittämiseen kehitettiin spektrofotometrinen menetelmä, joka perustuu ligniinin happamien hydroksyyliryhmien mittaamiseen kationisen väriaineen adsorptiolla neutraalissa vesisuspensiossa. Vehnän oljesta eristetyn alkalilignniinin happamien hydroksyyliryhmien kokonaismäärästä noin puolet oli väriaineen saavutettavissa, minkä tulkittiin johtuvan ligniinin avaruusrakenteesta.

Autohydrolyysin vaikutus vehnän oljen ligniinin rakenteeseen selvitettiin esikäsittelyn severiteetin funtiona. Kemialliset ja kromatografiset analyysit vahvistivat, että ligniini pilkkoutui sekä autohydrolyysin että tämän jälkeisen korkean intensiteetin alkalisen uuton vaikutuksesta. Havaittiin ligniinin pinta-alan pienentyvän autohydolyysin voimakkuuden funktiona sekä esitettiin tämän johtuvan ligniini-hiilihydraattiverkoston happokatalyyttisen hydrolyysin aiheuttamasta ligniinin rakenteen tiivistymisestä. Eräs päätuloksista oli osoitus ligniinin pinta-alan käänteisestä korrelaatiosta selluloosan entsymaattisen hydrolyysiasteen kanssa. Tämän uuden tiedon hyödyntäminen johtanee ligniinin pinta-alan tavoiteltuun pienentämiseen esikäsittelyprosesseissa.

Avainsanat Ligniini, rakenne, lignoselluloosa, selluloosa, entsymaattinen hydrolyysi

ISBN (painettu) 978-952-60-6234-1 **ISBN (pdf)** 978-952-60-6235-8

ISSN-L 1799-4934 **ISSN (painettu)** 1799-4934 **ISSN (pdf)** 1799-4942

Julkaisupaikka Helsinki **Painopaikka** Helsinki **Vuosi** 2015

Sivumäärä 128 **urn** http://urn.fi/URN:ISBN:978-952-60-6235-8

Preface

The work reported in this thesis was carried out at the Department of Biotechnology and Chemical Technology at Aalto University School of Chemical Technology (Finland) and at Institut Jean-Pierre Bourgin, INRA/AgroParisTech (France) during the years 2010–2015. The work in Finland was mainly funded by the BIOLI project in collaboration with Neste Oil Corporation. I would like to thank Perttu Koskinen and Jukka-Pekka Pasanen from Neste Oil for making it possible to conduct scientific research seamlessly within this engineering project. Additional financial support from The Emil Aaltonen Foundation, The Finnish Foundation for Technology Promotion, and Aalto University School of Chemical Technology is gratefully acknowledged.

I would like to express my deepest gratitude to my supervising Professor Simo Laakso for his trust, guidance, and encouragement that I have received. I feel fortunate for the possibility to work in his group and to absorb some of his broad experience in science, technology, and project leadership. Thank you for sharing this expertise and introducing me to the fascinating world of applied biochemistry.

My special thanks belong to my thesis advisor Ph.D. Ossi Pastinen for his patience, time, and support during my studies. There has not been a topic that he could not help elucidate thanks to his interdisciplinary experience in broad fields of chemistry. Our close collaboration has without doubt significantly shaped my thesis. Furthermore, I am equally grateful for my thesis advisor Professor Stéphanie Baumberger for the invaluable guidance and friendship during and after my exchange in the “Lignins and tannins” research group in Versailles. During this time I learned the essentials of chemistry and analysis of lignin also under guidance of Professor Catherine Lapierre. Thank you also for introducing some bits of the French culture and having patience with my oral French.

I am grateful for the constructive comments given by Docent Mats Galbe and Professor Raimo Alén who served as the pre-examiners of this thesis. I wish to thank sincerely the doctoral program planning officer Sirje Liukko for assistance in study affairs, and for guiding me through the university bureaucracy. I would also like to thank Professor Emeritus Matti Leisola for his support and interest in my studies.

Warm thanks go also to my co-authors and current and former colleagues in France and in Finland. I have been fortunate to collaborate with self-motivated and talented people like Ville Pihlajaniemi, Ilkka Lehtomäki, and the other LIGNOBOYS. Marjatta Vahvaselkä, Heidi Vainio, and Sanna Hokkanen have displayed the amazing world of microorganisms as cellular factories. In addition to the work responsibilities in the Biochemistry Research Group, it has been great to enjoy the tasty dishes during our frequent cooking evenings (with the exception of the fermented herring). The spirit within the group has been

excellent, and it has been great to share the ups and downs as well as the hilarious lobster and fish tag emails with you.

I wish to extend my heartfelt thanks to my family, relatives and friends. I warmly thank my parents Heikki and Leenamaija for the unconditional love and support that you have given throughout my life. My warm thanks go also to my little brother Matias and to my older sister Mari and her family, for being around me.

Finally, I would like to dedicate this thesis to my loving wife Fei who in the first place encouraged me to start the doctoral studies. Our shared explorations of the world – near and far – have provided much-needed counterbalance and perspective to this undertaking.

Espoo, May 2015

Mika Sipponen

Contents

List of publications

This doctoral dissertation consists of a summary and of the following publications which are referred to in the text by their bolded Roman numerals. Additional unpublished data is also presented.

I Sipponen, M.H., Lapierre, C., Méchin, V., Baumberger, S. Isolation of structurally distinct lignin–carbohydrate fractions from maize stem by sequential alkaline extractions and endoglucanase treatment. *Bioresour. Technol.* **133** (2013) 522–528.

II Sipponen, M.H., Laakso, S., Baumberger, S. Impact of ball milling on maize (*Zea mays* L.) stem structural components and on enzymatic hydrolysis of carbohydrates. *Ind. Crops. Prod.* **61** (2014) 130–136.

III Sipponen, M.H., Pihlajaniemi, V., Littunen, K., Pastinen, O., Laakso, S. Determination of surface-accessible acidic hydroxyls and surface area of lignin by cationic dye adsorption. *Bioresour. Technol.* **169** (2014) 80–87.

IV Sipponen, M.H., Pihlajaniemi, V., Sipponen, S., Pastinen, O., Laakso, S. Autohydrolysis and aqueous ammonia extraction of wheat straw: effect of treatment severity on yield and structure of hemicellulose and lignin. *RSC Adv.* **4** (2014) 23177–23184.

V Sipponen, M.H., Pihlajaniemi, V., Pastinen, O., Laakso, S. Reduction of surface area of lignin improves enzymatic hydrolysis of cellulose from hydrothermally pretreated wheat straw. *RSC Adv.* **4** (2014) 36591–36596.

Author's contribution

I. The author MHS (Mika Henrikki Sipponen) defined the experimental plan together with the co-authors. MHS carried out the experiments including the analytical work. MHS interpreted the results and wrote the article together with the co-authors.

II. The author MHS defined the experimental plan together with the third author. MHS carried out the laboratory work, and interpreted the results and wrote the article jointly with the co-authors.

III. The author MHS defined the experimental plan and conducted the adsorption experiments and composition analyses. The NMR analysis was performed jointly with Kuisma Littunen. MHS interpreted the results, developed the quantitative method, and wrote the article together with the co-authors.

IV. The author MHS designed and executed the experimental work together with the co-authors. MHS set up the lignin analytical procedures jointly with Ossi Pastinen. MHS interpreted the results and wrote the article together with the co-authors.

V. The author MHS defined the experimental plan together with the second author. MHS interpreted the results and wrote the article jointly with the co-authors.

The author MHS is the corresponding author in each of the Publications **I**–**V**.

List of abbreviations and symbols

AFEX	ammonia fiber explosion
AH	autohydrolysis
a_L	Langmuir equilibrium constant
ARP	ammonia recycled percolation
ATR-FTIR	attenuated total reflection Fourier transform infrared
BET	Brunauer–Emmett–Teller
CA	*p*-coumaric acid
C_e	equilibrium concentration
CBM	carbohydrate-binding module
CBU	cellobiose unit
CC	cell corner
CMC	carboxymethyl cellulose
CML	compound middle lamella
DDFA	dehydrodiferulate
DHP	dehydrogenative polymer
DM	dry matter
DP	degree of polymerization
ε	extinction coefficient
EDS	energy dispersive spectroscopy
EFR	extractive-free residues
EtV	ethyl vanillin
FA	ferulic acid
FPU	filter paper unit
G	guaiacyl
GAE	gallic acid equivalent
GAX	glucuronoarabinoxylan
GC	gas chromatography
GC/MS	gas chromatography coupled to mass spectrometry
H	*p*-hydroxyphenyl

HMF	hydroxymethylfurfural
HPAEC	high-performance anion exchange chromatography
HPLC	high-performance liquid chromatography
HPSEC	high-performance size-exclusion chromatography
IS	internal standard
KL	Klason lignin
LC	lignin-carbohydrate
LCC	lignin-carbohydrate complex
LCN	lignin-carbohydrate network
M_i	molecular weight
ML	middle lamella
$\bar{M}_n$	number average molar mass
MS	mass spectrometry
MWL	milled wood lignin
$\bar{M}_w$	weight average molar mass
N_i	number of molecules
NMR	nuclear magnetic resonance
PD	polydispersity
P	primary cell wall
q_e	equilibrium adsorption capacity
RI	refractive index
S	syringyl
S	secondary cell wall
SA	surface area
SEM	scanning electron microscopy
SSA	specific surface area
SGB	sugarcane bagasse
T_g	glass transition temperature
THF	tetrahydrofuran
VWD	variable wavelength detector
WS	wheat straw
X_m	maximum adsorption capacity

1 Introduction

Plant residues represent remarkable potential as raw material for production of precursor chemicals and second-generation biofuels. Many common crops such as all cereals belong to the family of true grasses (Harris and Hartley, 1976). The disadvantages of cereal straws as resources compared to wood are their low densities and seasonal and scattered availability (Smil, 1999). On the other hand, exploitation of globally available plant residues does not compete with food production from arable land (Perlack *et al.*, 2011). For example, 430000 metric tonnes of wheat straw could be sustainably collected per annum (Talebnia *et al.*, 2010).

A majority of the dry matter of crop residues is comprised of cellulose (30–55%), hemicelluloses (15–40%), and the phenolic polymer lignin (10–25%) that renders the plant cell walls resistant against biochemical decomposition (Fan *et al.*, 1987). As a consequence, energy-intensive processing is indispensable in a lignocellulosic biorefinery of the biochemical type. The entire process chain covers pretreatment of lignocellulose, enzymatic hydrolysis of carbohydrates, biochemical conversion of sugars, and product recovery. This thesis deals with the first two steps.

The high proportion of lignin in the plant is the major detrimental factor in the enzymatic hydrolysis of associated carbohydrates (Chen and Dixon, 2007). Unfortunately, lignin and carbohydrates are covalently interlinked in grasses, and the effects of a variety of physicochemical lignocellulose pretreatments on lignin structure have not been elucidated systematically. Therefore, information is also lacking regarding the effect of lignin structure on enzymatic hydrolysis of cellulose. Moreover, efforts are currently booming in using lignin in more sophisticated applications (Norgren and Edlund, 2014), where fit structural properties of lignin would be pivotal.

In order to frame the experimental work of this thesis, the literature review that follows builds on the structure of grasses from molecular to macromolecular level. The complex cell wall construction of grasses and structural factors limiting their chemical and enzymatic deconstruction will be presented.

1.1 Main components of lignocellulose

Cellulose is the most abundant plant cell wall polymer and the main component of grasses. Structurally, cellulose is a linear polysaccharide consisting of D-glucopyranose units linked by β-(1→4)-glycosidic bonds (Fig. 1). Crystalline

periods of cellulose are formed by adjacent chains which are stabilized by extensive inter- and intra-chain hydrogen bonding. The cellulose molecules build up elementary fibrils, which form microfibrils that organize further into microfibrillar bands and cell wall fibers. Further details of the conformation, packing, and morphology of cellulose are provided in the in-depth reviews (O'Sullivan, 1997; Zugenmaier, 2008). Native plant cellulose consists of two distinct crystalline forms, I_α and I_β allomorphs (Atalla and VanderHart, 1984). The crystalline regions are disrupted by disordered regions which are important initiation sites of enzymatic hydrolysis (Lynd *et al.*, 2002). Grass cellulose is smaller compared to wood cellulose whose degree of polymerization (DP) falls in the range 6000−10000 (Zugenmaier, 2008).

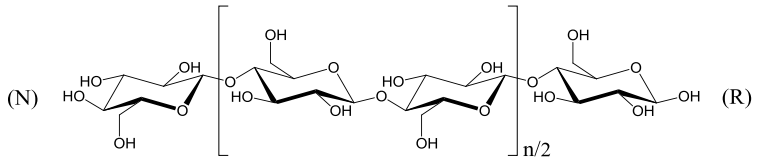

Figure 1. Molecular structure of cellulose showing the repeating cellobiose unit in square brackets. The non-reducing (N) and reducing (R) ends are indicated.

Glucuronoarabinoxylan (GAX) is the main grass hemicellulose (Ebringerová *et al.*, 2005). The main chain consists of D-xylopyranose units linked by β-(1→4)-glycosidic bonds, and is substituted with 4-*O*-methyl-D-glucuronic acid, L-arabinose, and acetyl groups (Nakamura *et al.*, 1993). Grass GAX contains ferulic acid (FA) ester-linked to C5 hydroxyl of arabinose moieties (Grabber *et al.*, 1995). A hypothetical partial structure of GAX is shown in Fig. 2a. Some of the adjacent GAX chains are interlinked via dehydrodiferulates (DDFAs, Fig. 2b), which comprise 0.01−0.05% of grass dry weight and render the grasses more rigid (Ishii, 1991; Iiyama *et al.*, 1994; Ralph *et al.*, 1994). Other hemicelluloses in primary (P) and secondary (S) cell walls of grasses in addition to GAX (P, 20−40%, S, 40−50%) are β-(1→3, 1→4)-glucan (P, 2−15%), glucomannan (P, 2%; S, 0−5%), and xyloglucan (P, 2−5%) (Scheller and Ulvskov, 2010). The weight average molar mass of grass hemicellulose usually falls in the broad range 50000−300000 g/mol, depending on the plant source and especially the isolation procedure used (Ebringerová *et al.*, 1992; Dervilly *et al.*, 2000).

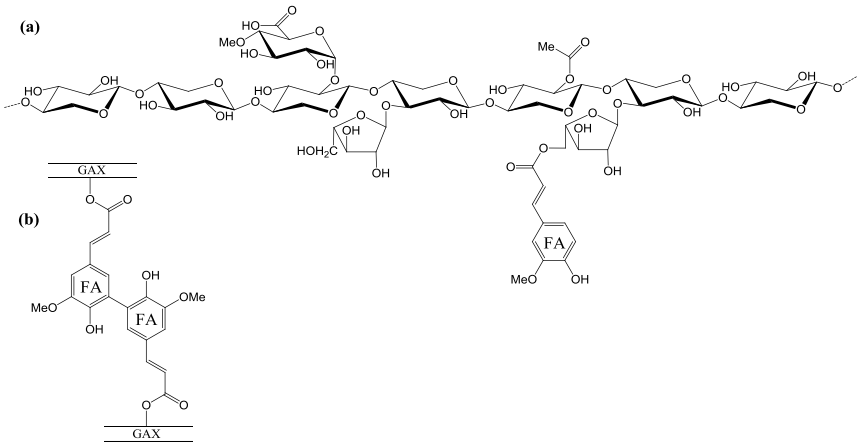

Figure 2. Partial molecular structure of grass glucuronoarabinoxylan (GAX) **(a)**. The xylan chain is partially acetylated at C2-*O*, and branched by arabinose α(1→3) and 4-*O*-methyl-D-glucuronic acid α(1→2). Ferulic acid (FA) is esterified to some of the arabinose moieties at C5 position. Adjacent GAX chains are cross-linked via dehydrodiferulate (DDFA) structures such as the one shown in **(b)**.

After cellulose, lignin is the second most abundant natural polymer and the main one based on aromatic units (Laurichesse and Avérous, 2014). Lignin is a term for the large group of branched aromatic polymers resulting from combinatorial oxidative coupling of 4-hydroxyphenylpropanoid moieties (Ralph *et al.*, 2004). Majority of lignin arises from three *p*-hydroxycinnamyl alcohols called monolignols biosynthesized by various enzymes which are needed in deamination, hydroxylation, and *O*-methylation of phenylalanine (Boerjan *et al.*, 2003). The three monolignols: *p*-coumaryl alcohol, coniferyl alcohol, and sinapyl alcohol give rise to *p*-hydroxyphenyl (**H**), guaiacyl (**G**), and syringyl (**S**) units of lignin (Fig. 3).

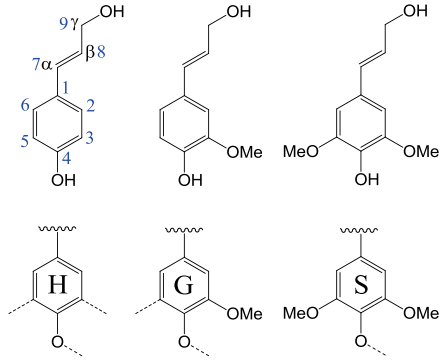

Figure 3. Lignin precursor monolignols *p*-coumaryl alcohol, coniferyl alcohol, and sinapyl alcohol (top row) and the corresponding *p*-hydroxyphenyl (**H**), guaiacyl (**G**), and syringyl (**S**) units of lignin. The aliphatic carbons 7–9 are referred to as α, β, and γ carbons, respectively, in this thesis.

Lignification is initiated by activation of the monolignols to reactive intermediates such as the quinone methide radical (structure II in Fig. 4) by enzymes such as laccases or peroxidases which induce dehydrogenative single electron abstraction. Polymerization of the activated intermediates occurs under chemical control by a series of radical coupling reactions which form carbon-carbon (C–C) bonds, referred to as condensed linkages, and weaker ether (C–O–C) bonds (Freudenberg and Neish, 1968; Sarkanen and Ludwig, 1971; Boerjan *et al.*, 2003).

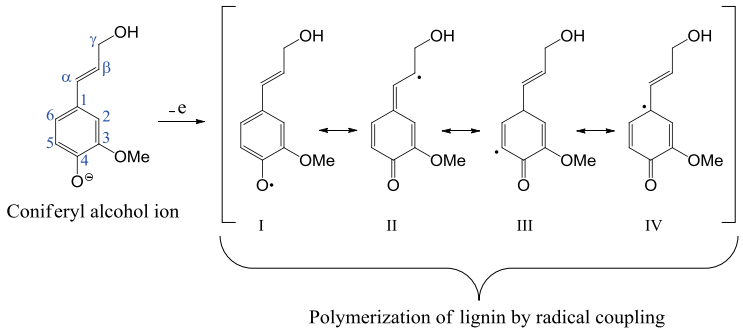

Figure 4. Single electron abstraction from dehydrogenated coniferyl alcohol generates the radical intermediates which form lignin by a series of coupling and dimerisation reactions (Freudenberg and Neish, 1968).

The typical linkage types of the lignin polymer are shown in Fig. 5. The β–O–4 aryl ether linkage is the most predominant bond type, accounting for more than half of the interunit connections (Adler, 1977; Dimmel, 2010). The minor α–O–4 linkage is incorporated in the dibenzodioxocin and phenylcoumaran ring structures (Crestini and Argyropoulos, 1997). In bamboo milled wood lignin (MWL) the α-O-4 linkages comprised 11% of the total number of aryl ethers (Higuchi *et al.*, 1972). Compared to the ether bonds, the condensed linkages 5–5, β–5, and β–β are stable in broader pH and temperature ranges.

Grass lignin is mainly composed of **G** and **S** units with lower proportion of **H** units. In addition to the natural variation due to botanical variance, the proportions of the structural units found depends on the analysis method; thioacidolysis, cupric oxide (CuO) oxidation, pyrolysis-GC/MS, and 2D nuclear magnetic resonance (NMR) spectroscopy of different wheat straw batches have given lignin H/G/S ratios of 4/42/54, 8/41/51, 16/50/34, and 7/52/41, respectively (Rolando *et al.*, 1992; Fidalgo *et al.*, 1993; Bocchini *et al.*, 1997; Yelle *et al.*, 2013). The presence of **H** units is a specific feature of grass lignin, since with the exception of softwood compression wood, lignin in wood does not contain significant proportion of **H** units (Rolando *et al.*, 1992). Other structural specificities of grass lignin are the high content of free phenolic groups (Lapierre *et al.*, 1989), and the frequent acylation of the aliphatic C_γ hydroxyl by *p*-coumaric acid (CA) (Ralph *et al.*, 2004).

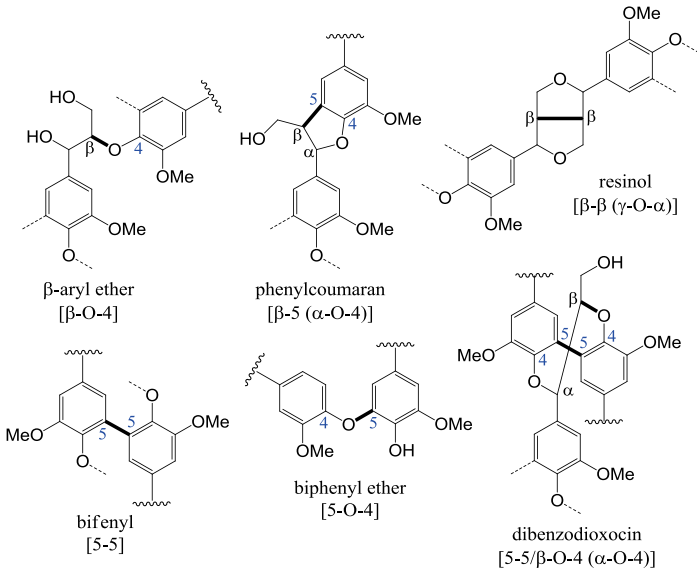

Figure 5. Major structural units of lignin polymer formed in the radical coupling (bolded bonds) and dimerization reactions. Redrawn from Ralph *et al.* (2004).

It was postulated almost 50 years ago that lignin isolated from wood according to the milled wood lignin method of Björkman (1956) might be less condensed than the bulk fraction of lignin in wood (Freudenberg and Neish, 1968). This hypothesis was only quite recently convincingly confirmed on wood (Crestini *et al.*, 2011). Generally, structure of lignin depends on the method used for its isolation, and lignin can be fractionated between solid and liquid phases in pretreatment. However, information is lacking of the possible fractionation of grass lignin linkage frequencies into solid and liquid fractions, even though alkaline pretreatment is a subject of renewed interest (McIntosh and Vancov, 2011; Pihlajaniemi *et al.*, 2015).

Lignin isolated from wheat straw and corn stover have given weight average molar masses in the range 1900−5900 g/mol when determined by high-performance size-exclusion chromatography (HPSEC) (Lawther *et al.*, 1996; Pakkanen and Alén, 2012; Monteil-Rivera *et al.*, 2013). These average molar masses and the associated polydispersities (*PD*=2.3−2.6) suggest that grass lignin is a rather small polymer which contains noticeable proportion of oligomers. It should be mentioned that HPSEC analysis of lignin is affected by the stationary and mobile phases used, calibration methodology, possible intermolecular associations, and co-elution of carbohydrates, lignin-carbohydrate complexes (LCCs) or impurities (Cathala *et al.*, 2003; Baumberger *et al.*, 2007). The view of the molecular structure of lignin has evolved with HPSEC, NMR, and other analytical techniques. Proposed structural models of softwood lignin and hardwood lignin in comparison to wheat straw lignin are shown in Fig. 6. Generally, the probability of branching in lignin increases as the proportion of **S** units decreases due to the lack of methoxyl substituent at C5 in the **G** units and their complete absence in the **H**

units. Hence, hardwood lignin (**GS**) and grass lignin (**HGS**) should be less branched than softwood lignin (**G**). Accordingly, a high proportion of the **H** units in grass lignin is linked via C−C linkages, as evidenced by the low amount of *p*-hydroxyphenyl units released in thioacidolysis of herbaceous straw (Rolando *et al.*, 1992). It is noted that the lignin model structures in Fig. 6 are simplifications of the so-called core lignin that does not adequately represent the native lignin bound to hydroxycinnamic acids and cross-linked with carbohydrates.

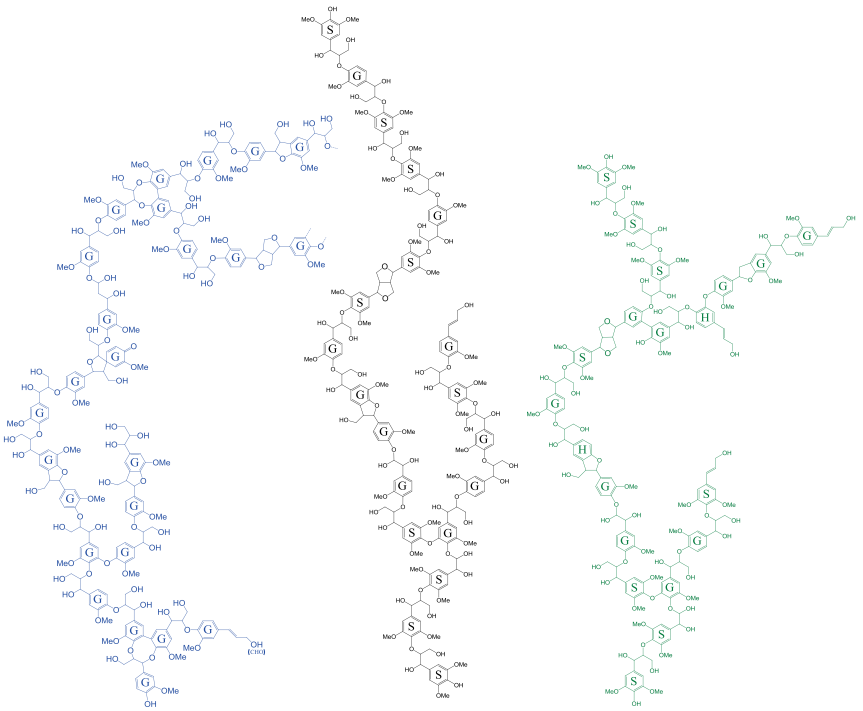

Figure 6. Models of lignin structure in: **(a)** softwood (spruce, **G**); **(b)** hardwood (poplar, **GS**), redrawn from (Ralph *et al.*, 2008); **(c)** wheat straw (**HGS**), drawn based on published structural information (del Río *et al.*, 2012; Yelle *et al.*, 2013). Average molecular weight of the monomeric unit and percentage elemental compositions of the models are: (a) 193 g/mol; C, 63.1; H, 6.1; O, 30.9 (b) 206 g/mol; C, 60.6; H, 6.1; O, 33.4 (c) 194 g/mol; C, 62.3; H, 6.0; O, 31.7.

1.2 Structure of grass stems and cell walls

Grass stems typically represent the largest proportion of the crop residues. Majority of grasses have a hollow stem (Fig. 7a), while in sugarcane and maize the stem is solid. Grass stems consist of numerous vascular bundles scattered in the ground tissue, which is surrounded by a strong and dense epidermis

(Fig. 7b) (Xu, 2010). Grass and wood materials have similar cell wall regions comprising middle lamella (ML) and cell corner (CC) regions surrounding the actual cell wall layers: primary (P) and secondary (S) wall and its three layers (S1, S2, and S3) (Côté, 1967; Xu, 2010) (Fig. 7c−d). Grass cell walls differ from those of wood mainly in thickness and volume of the regions. For instance, the S1 layer of wheat straw is thicker and the ML and the CC occupy higher volume than in spruce wood (Xu, 2010).

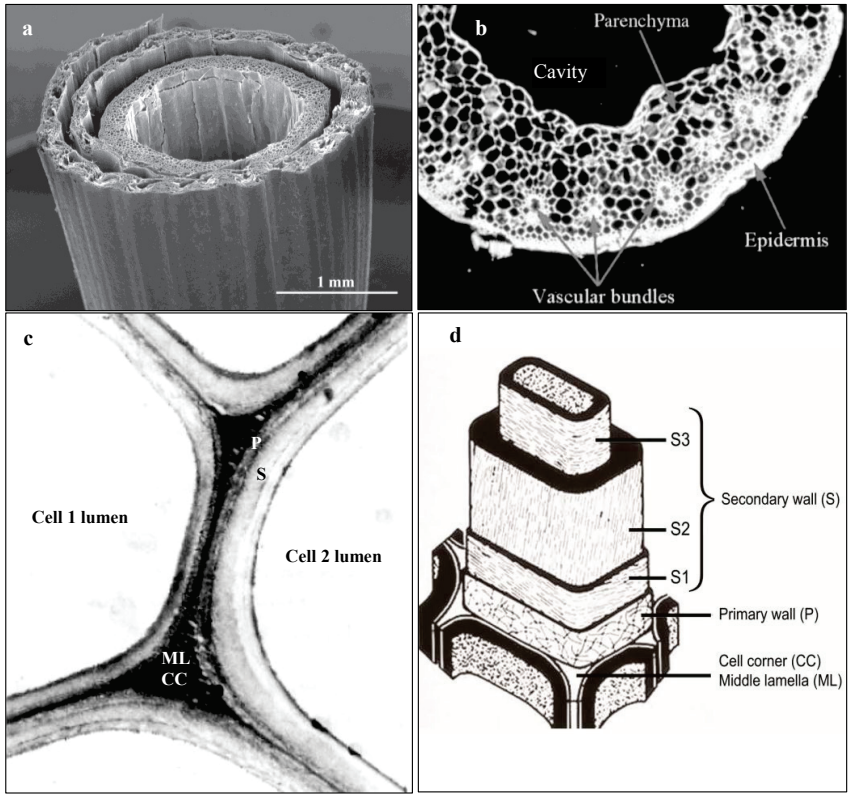

Figure 7. Visualisation of **(a)** wheat straw cross-section in scanning electron micrograph (SEM) (Kristensen *et al.*, 2008); **(b)** wheat straw transverse section in polarized optical microscopy, modified from Liu *et al.* (2005); **(c)** detailed view of wheat straw cells at 6000 × magnification of transmission electron micrograph showing cell wall layers, modified from Zhai and Lee (1989); **(d)** schematic representation of the mature wood cell wall layers, modified from Côté (1967).

The distribution of lignin in plant materials has been a central research area for decades, but the quantitative information exists mainly on wood. The approximate distribution of the main components of wood cell walls is shown in Fig. 8 (Hale, 1969). Compound middle lamella (CML) is highly enriched in lignin, but the proportion decreases rapidly in P and S1 layers. Thereafter, S2 and S3 contain around one fifth of lignin. Similarly, lignin concentration in wheat straw cell walls is the highest in the cell corner (CC) and lowest in the

S2 (Xu, 2010). Zhai and Lee (1989) reported 57−66% lignin concentration in the CC, 34−41% in the ML and 15−16% in the S2 using bromination in conjunction with energy dispersive spectroscopy (EDS). Lower lignin concentrations of 31% in the ML and 9% in the S2 of wheat straw were found by interference microscopy (Donaldson *et al.*, 2001). Most of the parenchyma cells were lignified except for a few cells lining the stem cavity. The comparability of the lignin distribution data obtained using different analytical techniques was called into question (Donaldson *et al.*, 2001). It is nevertheless apparent that the highest proportion of the total lignin content of wheat straw is located in the ML and CC, which is consistent with the fact that over 50% of the grass lignin is soluble in dilute alkali at room temperature (Lapierre *et al.*, 1989) and as much as 80% after one hour extraction of wheat straw with NaOH at 140 °C (Pihlajaniemi *et al.*, 2015). At the grass stem transverse section level, the lignin concentration is the lowest in the epidermis cells of wheat straw (Xu, 2010). In contrast, Donaldson *et al.* (2001) observed strong fluorescence in the epidermal cells of wheat straw, which would indicate high lignin concentration, but autofluorescence of cutin could not be ruled out. Possible interference from cutin was not mentioned in a study where lignin staining and image analysis suggested that maize stem epidermis was enriched in lignin (Zhang *et al.*, 2013a). Advanced confocal and fluorescence microscopy techniques are expected to shed further light on distribution of lignin and changes caused during the lignocellulose pretreatment process (Coletta *et al.*, 2013). In addition to lignin distribution, association of the main structural polymers is a crucial feature which governs many properties of lignocellulose in pretreatment and biochemical conversion of carbohydrates.

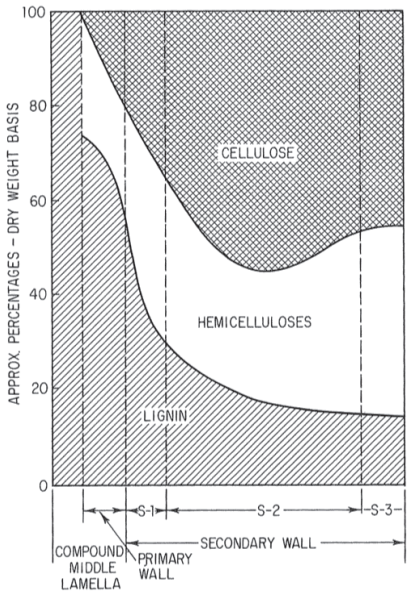

Figure 8. Approximate distribution of lignin, hemicelluloses, and cellulose in wood cell wall (Hale, 1969).

1.3 Association of the main components

Grass secondary cell walls consist of cellulose microfibrils embedded in a reinforcing network of hemicelluloses and lignin (Fig. 9). Associations and covalent bonds between these components cause challenges for enzymatic deconstruction of the composite structure of cell walls and for separation of the main components (Balakshin *et al.*, 2011). The difficulty of isolating pure carbohydrates or lignin arises in the first place from the physical association and cumulative weak interactions between the molecules. Secondly, lignin and carbohydrates are covalently linked in LCCs, whose components cannot be separated without breaking lignin-carbohydrate (LC) linkages (Björkman, 1957). Isolation of LCCs from wood for analysis requires multi-stage processes comprising milling, extraction and purification steps (Lawoko, 2005). Direct covalent linkages between cellulose and lignin have been proposed in wood, but cross-links between hemicellulose and lignin are more frequent especially in grasses (Grabber *et al.*, 2004).

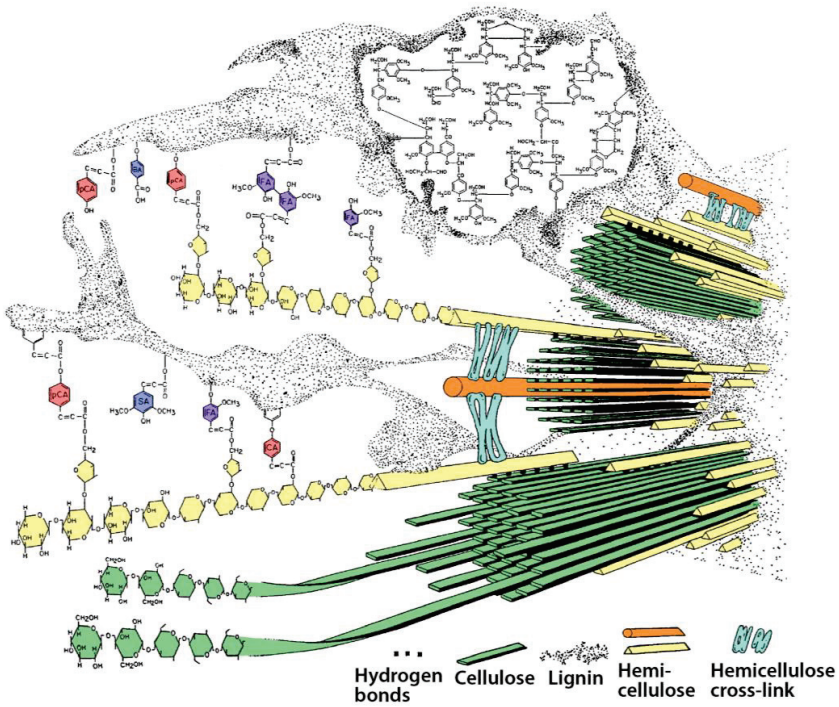

Figure 9. A model of the grass secondary cell wall showing association of the main structural components. Modified from Bidlack *et al.* (1992).

The network surrounding cellulose is comprised of hemicellulose and lignin, and is referred to as lignin-carbohydrate network (LCN) (Guerra *et al.*, 2006). In grass LCN, lignin and GAX are interconnected for instance via FA esterified to GAX and etherified to lignin, as experimentally evidenced (Jacquet *et al.*,

1995). Pioneering identification and quantification of the LC linkages have been achieved by comparative wet chemistry analyses using model compounds (Koshijima and Watanabe 2003), and more recently by quantitative NMR spectroscopy (Balakshin *et al.*, 2011). The accumulated structural information is consistent with the LC linkages proposed by Iiyama *et al.* (1994) (Fig. 10). The existence of LC linkages has also important technical consequences. Hydrolysis of the LC ester linkages explains the high solubility of grass lignin in dilute alkali (Grabber *et al.*, 2004). In contrast to the prevalent ester linkages, the ether bonds between lignin and hemicelluloses are more stable. It is also important to note that when the ester linkage of the FA bridge interconnecting hemicelluloses and lignin is cleaved, the lignin component retains the etherified FA with a free carboxylic group. The general consequence of the LC linkages is that grasses are biochemically recalcitrant regarding both enzymatic hydrolysis and digestibility as forage (Jeffries, 1990; Cornu *et al.*, 1994).

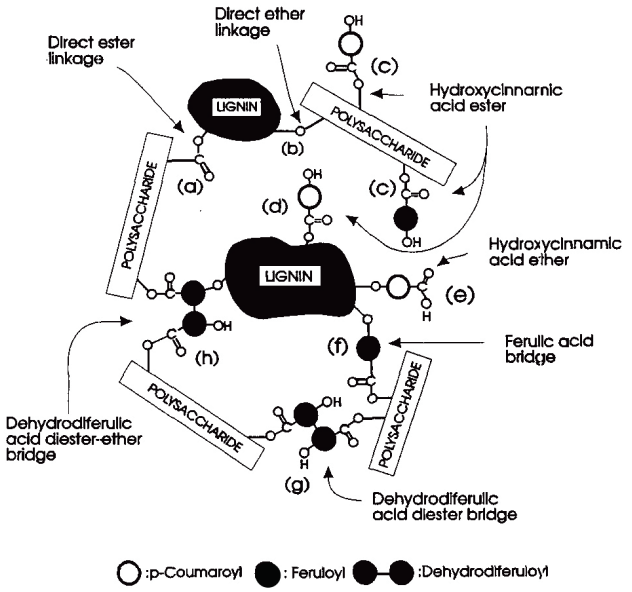

Figure 10. Possible covalent linkages between lignin and carbohydrates in plant cell walls (Iiyama *et al.*, 1994).

1.4 Overview of lignocellulose pretreatment processes

Various different pretreatment technologies have been developed for overcoming recalcitrance of lignocellulose towards hydrolytic enzymes, and the progress in the field has been frequently reviewed (Alvira *et al.*, 2010; Galbe and Zacchi, 2012; Mood *et al.*, 2013; Behera *et al.*, 2014). Pretreatments can be divided, for instance, to thermal, chemical, and mechanical treatments, and their combinations. In this thesis, pretreatments are further categorized to

acidic, neutral, and alkaline processes based on their prevailing pH. Hydrolysis of ester and glycosidic bonds occurs in acidic pretreatments, whereas in mild alkaline conditions mainly ester bonds are cleaved resulting in dissolution of lignin and hemicellulose.

Common pretreatments include hydrothermal, dilute acid hydrolysis, acidic sulfite treatment, ammonia fiber explosion (AFEX), ammonia recycled percolation (ARP), organosolv and alkaline hydrolysis or wet oxidation processes (Table 1). In contrast to the chemical pulping processes optimized for production of high quality cellulosic fibers, pretreatments pursue higher solids yield and remove less lignin from the biomass. Partial depolymerization or reduction of crystallinity of cellulose might also occur as a result of pretreatment and turn out beneficial for the enzymatic hydrolysis reaction. Nevertheless, pretreatment severity should be controlled in order to avoid inordinate generation of degradation products that inhibit bioconversion of sugars (Palmqvist and Hahn-Hägerdal, 2000). Pretreatments have been mainly optimized on the basis of enzymatic digestibility of the processed solid fraction, but total sugar yield from wheat straw was recently related to enzyme productivity and recommended as the basis of assessment of different pretreatments (Pihlajaniemi *et al.*, 2015). A commercially viable lignocellulose pretreatment process should additionally involve low capital and operational expenditures and the possibility for energy and steam re-use (Galbe and Zacchi, 2012). Based on these criteria dry fractionation and related methods relying solely on mechanical particle size reduction are not economically feasible pretreatment processes for lignocellulosic materials (Hendriks and Zeeman, 2009; Barakat *et al.*, 2013). Moreover, biological pretreatments are inefficient (Talebnia *et al.*, 2010) and were thus excluded from this work in addition to methods which have not been demonstrated beyond lab-scale such as treatments with ionic liquids.

Table 1. Major types of pretreatments, the typical process temperatures and the type of catalysts used.

Pretreatment type	Temperature (°C)	Chemical catalyst	Selected reference
Mechanical (milling)	20–100	Optional (acid or base)	Hideno *et al.*, 2009
Autohydrolysis	160–240	Optional (acid)	Overend and Chornet, 1987
Steam-explosion	160–240	Optional (acid, SO_2 or base)	Montané *et al.*, 1998
Dilute acid hydrolysis	140–200	Acid (H_2SO_4, HCl)	Esteghlalian *et al.*, 1997
Sulfite treatment	160–200	Acid, Na_2SO_3	Zhang *et al.*, 2013b
Organosolv	80–220	Organic solvent (acid or base)	Mesa *et al.*, 2011
AFEX[a]	< 100	NH_3 (g)	Dale *et al.*, 1996
ARP[a]	150–170	NH_4OH	Kim and Lee, 2006
Wet oxidation	150–200	Base (NaOH, KOH, $Ca(OH)_2$, NH_4OH)	Schmidt and Thomsen, 1998
Alkaline extraction/ delignification	20–160	Base (NaOH, KOH, $Ca(OH)_2$, NH_4OH)	McIntosh and Vancov, 2011

[a]: AFEX refers to ammonia fiber explosion, and ARP to ammonia recycled percolation.

Thermochemical (Abengoa, USA) and hydrothermal processes (BioChemtex, Italy; Raizen/Iogen, Brazil) are the major pretreatment technologies in cellulosic ethanol production which is currently the preprominent industrial lignocellulosic biorefinery. Hydrothermal pretreatments using steam and hot water are catalyzed by organic acids released from the feedstock at temperatures 160−240 °C (Garrote *et al.*, 1999; Galbe and Zacchi, 2012). One important example of the hydrothermal pretreatments is the autohydrolysis (AH) process which releases mainly water-soluble oligomers of hemicellulose (Carvalheiro *et al.*, 2009). AH without addition of acid is a rather mild acid hydrolysis since the starting pH is almost neutral and the pH at the end of the process is between 3.5–4 (Galbe and Zacchi, 2012).

Pretreatments deconstruct composite structure of cell walls essentially by disrupting the LCN. The most essential changes with respect to lignin are dissolution and depolymerization which may occur in reactions catalyzed by base or acid (Kondo *et al.*, 1987; Lundqvist, 1992a). Solubilization of lignin is also the target of industrial cellulosic pulp production wherein soda and sulfate cooking cause base catalyzed cleavage of aryl ether linkages at temperatures above 160 °C, whereas sulfonation of lignin is the most prominent reaction in acidic, neutral, or alkaline sulfite cooking at 140−170 °C (Lora, 2008). Water-soluble lignosulfonates are also released in sulfite pretreatment which is an effective process for wood (Shuai *et al.*, 2010), whereas SO_2 impregnation is a better suited option for agricultural residues (Geddes *et al.*, 2011). By analogy to the commercial scale processes, analytical degradations rely on cleavage of lignin in alkaline and acidic conditions (Lundqvist, 1992a; Chen, 1992; Rolando *et al.*, 1992). A majority of the at least 28 different phenolic compounds formed in acidolysis of lignin originate from scission of β-O-4 structures (Lundqvist, 1992a), which have been suggested to degrade also during steam pretreatment of wheat straw (Heiss-Blanquet *et al.*, 2011). Despite the fact that water-soluble lignin is released during AH, mainly the depolymerization of hemicellulose has been a subject of detailed investigations (Garrote *et al.*, 2001; Nabarlatz *et al.*, 2004). Presently, structural changes in lignin as a function of severity of hydrothermal or other acid-catalyzed pretreatments are not firmly established. Furthermore, degradation of lignin during ball milling of wood has been suggested (Guerra *et al.*, 2006), but experimental validation of this with grass lignin is lacking.

1.5 Enzymatic hydrolysis of lignocellulosic carbohydrates

Lignocellulosic carbohydrates can be hydrolyzed to monomeric sugars by acid hydrolysis or enzymatic hydrolysis. In contrast to acid hydrolysis processes which suffer from corrosion problems, sugar degradation, and expensive chemical recovery (Fan *et al.*, 1987; Sun and Cheng, 2002), enzymes hydrolyze lignocellulosic carbohydrates to monomeric sugars under mild reaction conditions. Enzymatic hydrolysis of grass GAX necessitates various

different activities including endoxylanases (EC 3.2.1.8), β-xylosidases (EC 3.2.1.37), α-L-arabinofuranosidases (EC 3.2.1.55), α-D-glucuronidases (EC 3.2.1.139), acetyl xylan esterases (EC 3.1.1.72), and feruloyl esterases (EC 3.1.1.73).

Cellulases hydrolyze β-(1→4) glycosidic bonds of cellulose. There are both noncomplexed and complexed cellulolytic enzyme systems (Lynd *et al.*, 2002). The former consists of three types of extracellular enzymes. Endoglucanases (EC 3.2.1.4) produce new free ends in the polymeric cellulose. Exoglucanases (EC 3.2.1.74) release cellodextrins and D-glucose from the cellulose chain ends. This group comprises also cellobiohydrolases (EC 3.2.1.91) which liberate D-cellobiose in a processive manner from the glucan chains. Soluble cellodextrins and cellobiose are hydrolyzed to D-glucose by β-glucosidases (EC 3.2.1.21) (Lynd *et al.*, 2002). Commercial cellulase production exploits mainly the filamentous fungi *Trichoderma reesei*, genetically engineered to produce up to 0.33 g of protein per gram of utilizable carbohydrate (Esterbauer *et al.*, 1991; Lynd *et al.*, 2002).

Complexed cellulases or cellulosomes are produced by anaerobic bacteria such as the thermophilic bacterium *Clostridium thermocellum* (Bayer *et al.*, 1983). Cellulosomes are cell wall-associated enzyme systems with high affinity for hydrolysis of crystalline cellulose. Initial hydrolysis occurs on the external cell surfaces, and the released soluble cellodextrins and cellobiose are taken up and hydrolyzed intracellularily to glucose-1-phosphate and D-glucose (Schwarz, 2001). One advantage of the cellulosome is the alignment of up to 11 different enzymes on the non-catalytic scaffold protein which ensures correct ratio of the catalytic components and high local sugar concentrations (Schwarz, 2001). From the biochemical production perspective, intracellular release of glucose is a disadvantage of the cellulosome system unless the same bacterial strain can be used as the production host.

Although the essential catalytic mechanisms have been established, recent discoveries suggest that our understanding of the cellulolytic systems is not yet complete. In fact, proteins catalyzing both hydrolysis and oxidation of cellulose were recently identified (Forsberg *et al.*, 2011). Moreover, swollenin, expansin and other non-catalytic proteins may enhance enzymatic hydrolysis of cellulose (Saloheimo *et al.*, 2002; Kim *et al.*, 2009). However, the auxiliary effects in hydrolysis of pure cellulose occurred only when cellulose dosages were lower than those required with lignocellulosic substrates. Lignocellulose suspensions from industrial pretreatment processes are demanding media for hydrolytic enzymes. Here, opportunities exist especially in improving thermal and pH stability of enzymes (Turunen *et al.*, 2002). Even though various pretreatments increase availability of the substrates to enzymes, residence time in enzymatic hydrolysis (24−96 h) is longer than in acid hydrolysis (2 h in a typical analytical procedure). Enzyme consumption is another challenge of the hydrolysis process (Pihlajaniemi *et al.*, 2014), as the percentage cellulose conversion increases linearly with logarithm of enzyme units used per gram of the initial substrate (Ghose, 1987). Furthermore, the possibility to recycle

enzymes is limited due to inactivation, adsorption on solid residues, and laborious separation of enzymes from water-soluble sugars. A near-term target price of hydrolytic enzymes in lignocellulosic ethanol production was approximately 0.05–0.10 €/dm^3 EtOH (Lynd *et al.*, 2008; Binder and Raines, 2010), which represent 15–30% of the current spot price of fuel-grade ethanol (Anon, 2015). Further cost reduction of the enzymatic hydrolysis step would therefore be pivotal.

1.6 Recalcitrance of lignocellulose towards enzymatic hydrolysis

Susceptibility of the natural composite lignocellulose to enzymatic hydrolysis depends on several factors including the degree of cellulose crystallinity, specific surface area of cellulose, porosity, accessible surface area and the presence of lignin. These and other factors influencing enzymatic digestibility of lignocellulosic carbohydrates have been categorized to direct and indirect factors (Zhao *et al.*, 2012). The biomass recalcitrance can be also viewed at three levels (1) whole plant and its anatomical regions, (2) proportions and structures of hemicelluloses and lignin, and (3) structure of cellulose (Fig. 11). This division is based on the view that the energy required for modifying the properties in each of these levels increases and the size of the structural units decreases in the listed order. The degree of crystallinity and specific surface area (SSA) are the most important substrate characteristics of cellulose limiting its hydrolysis (Mansfield *et al.*, 1999), but it is difficult if not altogether impossible to alter these traits without affecting the features in the above two levels. Likewise, delignification may affect properties above and below the second level.

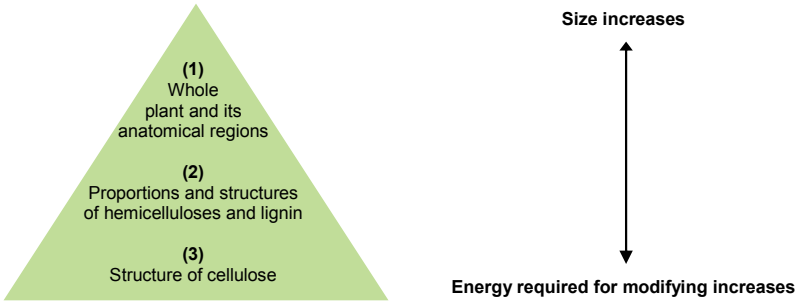

Figure 11. Three level of factors building up recalcitrance of lignocellulosic biomass towards enzymatic deconstruction.

At the first level shown in Fig. 11, epidermis tissue and its external surface comprising the cuticle, epicuticular waxes, and inorganic materials protect the plant from water loss, temperature variation, and attack of insects (Himmel *et al.*, 2007, Alvira *et al.*, 2010). The high content of silicon in the outer epidermis provides mechanical strength and microbial resistance (Zhai and

Lee, 1989; Xu, 2010). Besides the different features across the plant intersection, properties of grasses vary with growth stage and anatomical section of the plant (Boon *et al.*, 2012; Zhang *et al.*, 2013a). Nodes for instance are more resistant to hydrolysis than internodes in stems. Density and arrangement of pits and vascular bundles are important because they control diffusion of water into the tissues (Himmel *et al.*, 2007). In sugarcane stalk, vascular bundles are more lignified and recalcitrant than surrounding cells (Siqueira *et al.*, 2011). In wheat straw, the predominant adherence of cellulases changed from parenchyma cells to epidermal cells after hydrothermal pretreatment (Hansen *et al.*, 2013). Porosity is another important feature of lignocellulose since it governs the surface area accessible to microbes or their hydrolytic enzymes. In sugarcane stalk, cell walls from top internodes absorbed more water and were more porous and less lignified compared to lower parts of stalk (Maziero *et al.*, 2013). Pretreatments increase porosity and consequently the total surface area of the material which correlate with the rate of enzymatic hydrolysis (Gharpuray *et al.*, 1983; Thompson *et al.*, 1992). However, carbohydrate digestibility after dilute acid pretreatment of corn stover did not correlate with the total pore volume (Ishizawa *et al.*, 2007).

At the second level, hemicelluloses and lignin limit accessibility of hydrolytic enzymes on their substrates (Fig. 11). Lignin itself impedes digestibility of forages (Jung *et al.*, 1997) and dilute acid pretreated alfalfa stems (Chen and Dixon, 2007), as judged on the basis of negative correlation to lignin content. This detrimental effect has been attributed to inhibition of enzymes by lignin, irreversible adsorption of cellulases on lignin, and physical barrier from lignin or LCCs (Fan *et al.*, 1982; Jeffries, 1990; Sewalt *et al.*, 1997). A molecular basis for this impeding effect of lignin arises also from the LC linkages which cannot be completely cleaved by enzymes (Jeffries, 1990). While biosynthesis of lignin cannot be fully downregulated without negative changes in plant, genetic alteration of molecular structure of lignin could improve delignification potential of the plant raw material (Méchin *et al.*, 2014). However, it would be important to assess the feasibility of the modified plants as biorefinery raw materials by systematic pretreatment and enzymatic hydrolysis procedures. More consistent investigations combining the pretreatment mass balances and the effect of resulting grass lignin on enzymatic digestibility of carbohydrates would be valuable. Prior to the current work, the interactions of lignin and hydrolytic enzymes have been studied using isolated lignin and lignin derivatives, synthetic lignin dehydrogenative polymers (DHPs) and constructed thin films and cell wall model materials (Hoeger *et al.*, 2012; Rahikainen *et al.*, 2013; Martín-Sampedro *et al.*, 2013; Paës *et al.*, 2013; Li *et al.*, 2014). Concerning the structure of lignin, DHPs of the **H**, **G**, and **S** type had similar inhibitory effects on enzymatic hydrolysis of maize cell walls (Grabber *et al.*, 1997). One recent work reported qualitative changes in lignin distribution after phloroglucinol staining of hydrothermally pretreated wheat straw (Holopainen-Mantila *et al.*, 2013). However, direct quantitative investigations are scarce concerning the critical effect of

lignocellulose pretreatment on lignin structure and the consequences on enzymatic digestibility of carbohydrates. Presently, a firm relationship has not been established between the physicochemical structure of grass lignin and enzymatic digestibility of cellulose.

At the third level (Fig. 11), the intrinsic tightly packed and partially crystalline structure of cellulose protects it from enzymatic hydrolysis (Fan *et al.*, 1987; Mansfield *et al.*, 1999). Irreversible adsorption or reduced mobility on cellulose may further decrease productive activity of cellulases (Converse *et al.*, 1988; Igarashi *et al.*, 2011). Product inhibition and thermal inactivation of cellulases are inherent problems during the reaction (Mansfield *et al.*, 1999). While the non-catalytic carbohydrate-binding module (CBM) promotes recognition and association with the insoluble substrate (Boraston *et al.*, 2004; Bu *et al.*, 2009), removal of CBM from cellulases may decrease enzyme binding to lignin and consequently enhance enzymatic digestibility of lignocellulosic carbohydrates (Le Costaouëc *et al.*, 2013). The amount of cellulolytic enzymes required can be reduced by altering native crystalline structure of cellulose, but the downsides of this approach include industrially unattractive treatments in ionic liquids, anhydrous ammonia or concentrated sodium hydroxide (Zhao *et al.*, 2009; Gao *et al.*, 2013). Enhanced stability, activity and overall production processes of glycoside hydrolases are needed to improve the economic viability of the enzymatic hydrolysis of lignocellulosic carbohydrates. In the meanwhile, fundamental understanding is needed of the effect of various lignocellulose pretreatments on grass lignin structure to assess the consequences on enzymatic hydrolysis of cellulose and in order to develop more efficient biorefinery processes.

2 Aims of the thesis

The overall objective of this thesis is to elucidate structural changes that occur in grass lignin in various chemical, mechanical, and hydrothermal treatments of lignocellulose, and to use this information for assessing enzymatic digestibility of cellulose. To fulfil this objective, the research was targeted on the following subgoals:

- Determination of quantitative and qualitative fractionation of lignin structure during sequential alkaline extraction of grass lignocellulose.

- Assessment of the effect of mechanical treatment on structure of grass lignin and consequences on enzymatic hydrolysis of carbohydrates.

- Development of a method for determination of lignin surface area based on surface-accessible acidic hydroxyl groups in lignocellulose.

- Determination of the effect of autohydrolysis and alkaline extractions on chemical and physical structures of grass lignin, followed by elucidation of their impact on enzymatic hydrolysis of cellulose.

By satisfying the objective of the thesis, it is anticipated that the ground will be laid for the development of more efficient pretreatment processes for plant residues.

3 Materials and methods

The main experimental techniques and materials used are presented in this section. The reported results are mean values from duplicate experiments, unless otherwise indicated. More detailed information can be found in the original publications **I**–**V**.

3.1 Lignocellulosic materials[I–V]

The lignocellulosic materials used in **I**–**V** included agricultural plant residues milled to pass a 1 mm sieve: maize (*Zea mays* L.) stem, oat (*Avena sativa* L.) husks, sugarcane (*Saccharum officinarum* L.) bagasse (SGB), and wheat (*Triticum aestivum* L.) straw (WS). Commercial wheat straw soda lignin was purchased from GreenValue SA. WS lignin was isolated from WS soda black liquor originating from a two-step bench-scale process (5 h autohydrolysis at 140 °C followed by delignification in 1 M NaOH at similar conditions). The black liquor was precipitated with sulfuric acid and subjected to xylanase treatment at pH 5 in order to solubilize and separate hemicelluloses from insoluble lignin which was recovered by centrifugation. Whatman I filter paper (Sigma-Aldrich) and microcrystalline cellulose Emcocel 50M (Penwest Pharmaceuticals) were commercial products. Soxhlet extraction of plant material first with deionized water and then with ethanol was used to prepare extractive-free residues (EFR). Acetylation of lignin in pyridine:acetic anhydride (1:1, v/v) mixture and purification of the products were carried out according to the literature (Gosselink *et al.*, 2004). Compositions of the characterized materials are shown in Table 2.

3.2 Enzyme preparations[I–III, V]

Hydrolytic enzymes used in this work included commercial products Novozyme 476, Onozuka R-10, Econase CE, Novozyme 188, GC 140, and a purified endoxylanase PaXyn11A. Details of these enzyme preparations are given in Table 3. Protein contents of the preparations were assayed according the Bradford (1976) method using bovine serum albumin (Sigma) as standard. Hydrolytic activities were assayed following the literature procedures (Ghose, 1987; Nakamura *et al.*, 1993). The substrates, carboxymethyl cellulose (CMC), beech xylan, Whatman I filter paper, and cellobiose were purchased from Sigma-Aldrich.

Table 2. Composition of lignocellulosic materials used in **I–V**.

Material	Publication	Glc	Xyl	Ara	Gal	Ac	KL	ASL	Ash
Maize stem (EFR)	**I–II**	40.0	20.2	2.4	0.6‡	na[a]	17.3	1.5	na
Wheat straw	**III–V**	39.0	23.7	2.7‡	0.9‡	1.9	21.8	1.8	4.2
Sugarcane bagasse	**III**	40.8	22.4	2.1	0.8	3.0	22.0	1.8	3.0‡
Oat husks	**III**	31.0	31.4	3.1	1.3	2.7	20.4	2.4	4.6
Wheat straw (EFR)	**III**	38.4	23.3	3.0‡	1.2‡	1.8	20.0	1.4‡	5.1‡
WS lignin	**III**	nd[b]	0.8	0.2‡	nd	nd	79.2	3.7	4.0
GreenValue lignin	**III**	0.2‡	2.7	0.9	0.1‡	na	86.4	5.2	1.4
Whatman I	**III**	96.6	nd	nd	nd	na	0.8‡	0.3	na
Emcocel 50M	**III**	95.7	1.4‡	0.4‡	nd	na	nd	0.2	na

Carbohydrates are expressed as anhydrous sugar residues: Glc, glucose; Xyl, xylose; Ara, arabinose; Gal, galactose. Ac, acetyl groups; KL, Klason lignin; ASL, acid-soluble lignin. EFR, extractive-free residues. [a]: na, not analyzed; [b]: nd, not detected. Composition results are mean values of duplicate experiments, with average deviation relative to the mean < 5%, unless marked with the ‡ symbol.

Table 3. Properties of hydrolytic enzyme preparations used in **I–III** and **V**.

Enzyme	Publication	Protein concentration [mg/ml][a]	Main activity	Activity on substrate [U/ml]	Source[b]
Novozyme 476	**I**	6.7 ± 0.3	Endoglucanase	CMC: 107; Beech xylan: 1.6	(A)
Onozuka R-10	**II**	89 ± 3 [mg/g][c]	Cellulase preparation	CMC: 2.65; Beech xylan: 80.1 [U/mg][d]	(B)
PaXyn11A	**II**	6.6 ± 0.2	Purified endoxylanase	Beech xylan: 32.4	(C)
Econase CE	**V**	35.6 ± 0.9	Cellulase preparation	Whatman I filter paper: 37.0	(D)
Novozyme 188	**V**	23.9 ± 0.5	β-Glucosidase	Cellobiose: 1262 [CBU/ml]	(E)
GC 140	**V**	8.7 ± 0.3	Xylanase preparation	Birch xylan: 1040	(F)

One unit of activity (U) refers to the amount (μmol) of xylose or glucose released from the substrate by the enzyme in 1 min under the assay conditions. [a]: Reported as mean value ± average deviation of duplicate experiments. [b]: (A) Novozymes, Denmark; (B) Serva Electrophoresis, Germany; (C) INRA/Marseille, France; (D) AB enzymes, Finland; (E) Sigma-Aldrich/Novozymes; (F) Genencor. [c]: mg of protein in g of the lyophilisate. [d]: activities per weight of the lyophilizate.

3.3 Sequential alkaline extraction, ball milling, and enzymatic hydrolysis of maize stem fractions[(I–II)]

Extractive-free maize stem (MS EFR) material was subjected to chemical and mechanical treatments in order to determine fractionation of lignin structure

that may arise from industrial pretreatments. MS EFR was extracted at room temperature in order to isolate lignin-containing fractions under mild thermal conditions (Fig. 12). The first extraction with 0.5 M NaOH and acidification of the liquid phase gave a fraction LC1. The solid fraction R1 was washed to neutral pH and hydrolyzed with Novozyme 476 (52.8 U/g) in 0.1 M Na-acetate buffer (pH 5) at 45 °C for 90 h. The solid fraction R2 was finally extracted with 2 M NaOH and LC2 obtained after acidification. The final solid residues R3 and the other fractions were characterized for composition and presence of hydroxycinnamic acids, and lignin structure was determined by thioacidolysis.

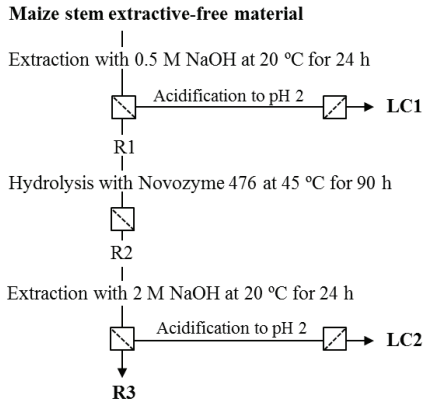

Figure 12. Scheme showing fractionation of maize stem extractive-free material into alkali-soluble lignin-carbohydrate fractions LC1, LC2, and solid residues R1–R3 (**I**).

Ball milling was carried out by weighing 3.0 g of MS EFR into a 50 ml stainless steel vessel with internal agate surface, and loaded with 28.6 g of agate balls (20 balls, 10 mm diameter). The vessel was fixed into a Retsch PM 100 planetary ball mill, operated at 600 rpm frequency at room temperature for a predetermined time with 20 min–20 min work–pause sequence. The actual working time of the mill excluding the paused time is presented in this work.

Enzymatic hydrolysis of lignin-carbohydrate fractions (LC1 and LC2 from **I**) and ball-milled maize stem materials was carried out at 1% or 2% dry matter consistency in 0.05 M Na-acetate buffer at pH 5. The 40 h and 72 h reactions catalyzed by PaXyn11A (33 mg protein/g solid material) or Onozuka R-10 (4.5 mg protein/g solid material) were conducted at 45 °C with continuous agitation. Sodium azide (Aldrich) was used in the reaction mixtures (0.025%) to prevent microbial contamination. At the end of the reaction, the suspension was centrifuged, and sugars were analyzed from the supernatant with high-performance anion exchange chromatography (HPAEC). The solid residues were washed three times with water and lyophilized. Single control experiments containing lignocellulosic materials without enzymes were carried out in parallel with the enzymatic treatments.

3.4 Adsorption of Azure B on lignin and crop residues[III]

Adsorption experiments were conducted by adding a predetermined amount of Azure B (Aldrich, USA) in aqueous solution into a conical flask or screw cork glass tube containing the adsorbent. The reactions were carried out in a thermostatic oven with continuous agitation. Contact time was 24 h, except in the kinetic experiments where contact time was from 1 min to 24 h and temperature 15 °C, 25 °C or 50 °C. The effect of pH was studied in 0.05 M buffer solutions at varying pH from 3 to 8. Adsorption data were used to determine parameters for the Langmuir (1916) isotherm (Eq. 1).

$$q_e = \frac{X_m a_L C_e}{1 + a_L C_e} \quad (1)$$

Here, q_e (mg/g) is the equilibrium adsorption capacity, X_m (mg/g) is the maximum adsorption capacity, a_L (dm^3/mg) is the Langmuir equilibrium constant, and C_e (mg/dm^3) is the equilibrium concentration. Surface-accessible acidic hydroxyl groups were calculated from Eq. 2, surface area (SA) of lignin from Eq. 3, and specific surface area (SSA) of lignin was calculated from Eq. 4.

$$\text{Surface-accessible acidic OH } \left(\frac{\text{mmol}}{\text{g material}}\right) = b \cdot \frac{X_m}{305.83} \quad (2)$$

$$SA = \text{Surface area of lignin } \left(\frac{\text{m}^2}{\text{g material}}\right) = \text{Surface-accessible acidic OH} \cdot 397 \quad (3)$$

$$SSA = \text{Specific surface area of lignin } \left(\frac{\text{m}^2}{\text{g lignin}}\right) = \text{SA/proportion of lignin} \quad (4)$$

Here, b is the correction factor (0.87−0.94) for non-specific binding of Azure B, 305.83 is the molar mass of Azure B (g/mol), 397 (m^2/mmol) is the area covered by Azure B, and proportion of lignin (%) is the sum of Klason lignin and acid-soluble lignin contents of the adsorbent. The area covered by protonated Azure B was calculated from its Connolly (1983) molecular surface area based on the assumption of spherical molecular geometry.

3.5 Autohydrolysis, alkaline extraction, and enzymatic hydrolysis of wheat straw[IV–V]

WS was subjected to AH only or AH with subsequent NH_3 (aq) extraction, as shown in Fig. 13 (**IV**−**V**). Aqueous suspension of WS at 10% consistency (g dry WS/g total) was prepared in deionized water. The suspension (210 g) was adjusted to pH 4.5 with 0.1 M acetic acid, and heated to a predetermined maximum temperature of 170−200 °C in a stirred (125 rpm) autoclave reactor. The reactor was cooled in an ice bath and the solid and liquid fractions were

separated by filtration for analysis. The temperature data on the treatment were recorded and used to calculate the severity parameter from Eq. 5, where $T(t)$ is the reaction temperature as a function of reaction time t (min) (Overend and Chornet, 1987).

$$R_0 = \int_0^t exp^{\frac{T(t)-100}{14.75}} dt \quad (5)$$

Solid residues from WS autohydrolysis were extracted at 5% consistency with 5% or 20% NH_3 (aq) (g NH_3/g liquid) by heating the suspension to 140 °C or 160 °C, respectively. The extracted solid residues were separated by filtration from the liquid phase, which was evaporated to dryness at 40 °C. The solid residues were washed with deionized water, pressed and stored at 4 °C. Each of the fractions was characterized for composition, and dry matter yield was determined from mass balances. Lignin structure in the solid residues and in the aqueous ammonia extracts obtained at 140 °C was characterized by alkaline CuO oxidation. The liquid fractions were additionally analyzed with HPSEC.

Each solid residue was subjected to enzymatic hydrolysis in aqueous Na-phosphate buffer at pH 5 using Econase CE (15 FPU/g) supplemented with GC 140 (1020 U/g) and Novozyme 188 (81 CBU/g). The reactions at 2% consistency and at 50 °C were conducted in capped glass flasks agitated in an oscillated water bath. Tetracycline (0.04 g/l) and cycloheximide (0.03 g/l) were used to prevent microbial growth. Monosaccharides in the liquid phase were analyzed with high-performance liquid chromatography (HPLC) after 24 h and 72 h reaction times.

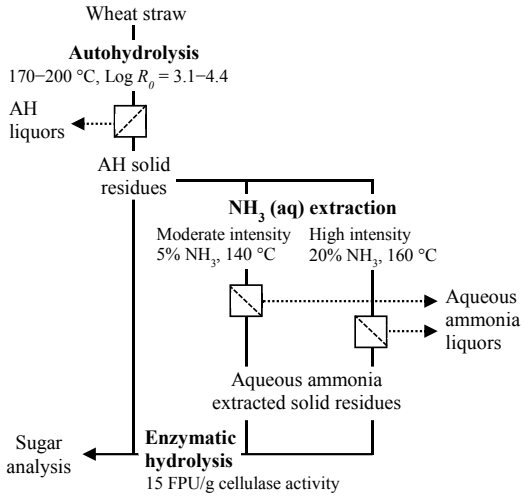

Figure 13. Scheme showing fractionation of wheat straw by autohydrolysis and NH_3 (aq) extraction before enzymatic hydrolysis of the solid residues (reproduced from **IV**−**V**).

3.6 Analytical procedures[I–V]

3.6.1 Composition analysis

Composition of lignocellulosic materials was analyzed on the basis of the two-stage sulfuric acid hydrolysis following the procedures adapted from Dence (1992) (**I**−**II**) or from Sluiter *et al.* (2010) (**III**−**V**). The acid-insoluble residue was corrected for its ash content and termed Klason lignin. Acid-soluble lignin was determined from the liquid phase based on UV-absorbance at 205 nm (ε=110 ml/(mg·cm)). Carbohydrates in isolated lignin or lignin-carbohydrate materials and in AH liquors (Fig. 13) were hydrolyzed in 4% sulfuric acid (w/w) at 121 °C for 1 h. Sugars were analyzed either as reducing sugars using the dinitrosalisylic acid procedure (Miller, 1959) or as monosaccharides with an HPAEC system comprising a CarboPac PA-1 column (Dionex) coupled to a pulsed amperometric detector ED 40 (Dionex) (**I**–**II**) or with an HPLC system comprising an SPO810 column (Shodex) coupled to a refractive index (RI) detector (Shimadzu) (**III**–**V**). In HPLC analysis, deionized water delivered at flow rate of 0.7 ml/min was used to elute the columns at 60 °C. Identification of the substances was based on retention times, and quantification on external standard calibration. Lignin content of the aqueous ammonia extracts was determined by UV-spectrophotometry. Mass extinction coefficient of the extract at 280 nm was converted to the percentage lignin content relative to GreenValue lignin (Table 2) (**IV**).

3.6.2 Analysis of decomposition products in autohydrolysis liquors

Water-soluble phenolic compounds in the autohydrolysis liquors were determined by the Folin–Ciocalteu method relative to gallic acid standards (Waterhouse, 2002). Furfural and hydroxymethylfurfural (HMF) were analyzed with the HPLC-RI system in identical conditions described in 3.6.1 for monosaccharide analysis. Formic acid, acetic acid, and levulinic acid were determined with an HPLC system comprising an Aminex HPX-87H separation column (Bio-Rad), and a type 2414 RI detector (Waters).

3.6.3 Alkaline hydrolysis

Ester- and ether-linked CA and FA were determined by mild and severe alkaline hydrolysis, respectively (Zhang *et al.*, 2011). Briefly, 50 mg of material was subjected to mild alkaline hydrolysis (2 M NaOH, 5 ml, 20 h at room temperature) or treatment at severe alkaline conditions in a polytetrafluoroethylene vial placed into an autoclave reactor (4 M NaOH, 5 ml, 2 h at 170 °C). The neutralized hydrolysates containing ethyl vanillin (EtV) as internal standard (IS) were analyzed after a purification procedure (Culhaoglu *et al.*, 2011) with HPLC equipped with a HyPURITY C18 column (Thermo) coupled to a photodiode array detector. The concentrations of CA and FA were

determined on the basis of their peak areas at 280 nm relative to EtV and pure substances in standard solution. The amounts of CA and FA detected after the mild hydrolysis were interpreted as esterified structures. The difference between the amounts of CA and FA obtained from the severe and mild alkaline hydrolyzes was interpreted as the amount of etherified structures.

3.6.4 Thioacidolysis

Thioacidolysis is an analytical method based on solvolytic cleavage of aryl ether linkages of lignin (Rolando *et al.*, 1992). Thioacidolysis of 10−20 mg of material was conducted in presence of heneicosane (IS), using 10 ml of the reagent consisting of boron trifluoride diethyl etherate (0.2 M) and ethanethiol (1.4 M) in dioxane solution. The reaction mixture in screw-cork glass tubes was placed in an oil bath set at 100 °C with occasional shaking during the 4 h reaction. The reaction mixture was neutralized with aqueous $NaHCO_3$ (0.4 M), extracted with dichloromethane, and the lignin-derived trithioethylated monomers were analyzed as their trimethylsilyl derivatives with gas chromatography (GC) coupled to mass spectrometry (MS) with an ion trap detector (Varian). The quantitative determination of **H**, **G**, and **S** monomers was performed from the ion chromatograms reconstructed at m/z 239, 269, and 299, respectively, as compared to the IS signal measured from the ion chromatogram reconstructed at m/z (57 + 71 + 85) (**I**).

3.6.5 Alkaline cupric oxide oxidation

Lignin structure was analyzed using alkaline cupric oxide (CuO) oxidation (Pepper *et al.*, 1967). The adapted procedure comprised heating aqueous ammonia extracts (25 mg) or solid residues (100 mg) in presence of CuO (500 mg) and 2 M NaOH (5 ml) in an autoclave reactor to 175 °C in 5 h before cooling to room temperature in 1 h. EtV was added as IS to the oxidation products which were quantitatively analyzed relative to external standard calibration with an HPLC system comprising a Nova-Pak C18 column (4 mm, 4.6 mm × 250 mm, Waters) and a variable wavelength detector (VWD) set at 280 nm. The mobile phase comprised mixtures of (A) water:formic acid (99.9:0.1, v/v) and (B) acetonitrile:formic acid (99.9:0.1, v/v) delivered at a flow rate of 0.8 ml/min. The gradient elution program started with 15 min isocratic step at 91% B, followed by a linear reduction of B to 83% at 28 min and further to 20% at 45 min.

3.6.6 High-performance size-exclusion chromatography

Thioacidolysis products were evaporated to dryness under nitrogen, fully dissolved in tetrahydrofuran (THF) stabilized with 3,5-di-*tert*-butyl-4-hydroxytoluene, and analyzed using an HPSEC system comprising a PLgel 5

μm MIXED-C pre-column (50 × 7.5 mm) and a chromatography column (600 × 7.5 mm, 100 Å) connected to a series of photodiode array and RI detectors. IGEPAL compounds from 4626 g/mol to 441 g/mol, guaiacyl dimer (β-5 GG), and coniferyl alcohol were used for relative calibration. Columns were eluted with the stabilized THF at room temperature at a flow rate of 1 ml/min. Lignin was analyzed with an HPSEC system comprising a series of three Ultrahydrogel size-exclusion columns (Waters), eluted with aqueous 0.1 M $NaNO_3$/0.01 M NaOH (Chen and Li, 2000). The column effluent was monitored with VWD (280 nm) and RI detectors (**IV**). Weight average molar mass ($\bar{M}_w$), number average molar mass ($\bar{M}_n$), and polydispersity (PD) were calculated based on the following equations relative to calibration constructed using poly(styrenesulfonate Na-salt) (Polysciences) and FA (Sigma) as standards (194000–194 g/mol).

$$\bar{M}_w = \frac{\sum M_i^2 N_i}{\sum M_i N_i} \tag{6}$$

$$\bar{M}_n = \frac{\sum M_i N_i}{\sum N_i} \tag{7}$$

$$PD = \frac{\bar{M}_w}{\bar{M}_n} \tag{8}$$

Here, M_i is the molecular weight of a detected molecule, and N_i is the number of molecules at that molecular weight.

3.6.7 Infrared spectroscopy

Maize stem fractions were characterized with attenuated total reflection Fourier transform infrared (ATR-FTIR) spectroscopy using a Nexus 470 spectrometer (American Nicolet Company). Averaged spectra from 5–10 individual acquisitions of each material with 10 scans were calculated. The crystallinity of cellulose was determined from the ratio of signal intensities at 1429 cm^{-1} and 894 cm^{-1} relative to the starting material MS EFR (O'Connor *et al.*, 1958).

3.6.8 CHN analysis and SEM-EDS

A Vario MAX elemental analyser (Elementar) was used to determine C, H, and N in WS lignin and GreenValue lignin. Wheat straw (**IV**) samples for SEM were coated with gold in Sputter Coater 108 auto (Cressington). SEM analysis was performed using a JSM-6610LV Scanning electron microscope (JEOL) comprising a Bruker 127 eV electron source in conjunction with EDS using an AXS Microanalysis system (Bruker).

3.6.9 UV-vis spectrophotometry

UV-vis spectra were recorded using quartz cuvettes in the wavelength region 200–500 nm. The spectra of WS lignin, GreenValue lignin, FA and CA were recorded in 0.1 M NaOH solution, and the spectra of CA and FA were also recorded in 0.05 M Na-phosphate buffer at pH 5. Beer-Lambert law ($A=\varepsilon cd$) was used to calculate the molar extinction coefficients (c has the unit [mmol/l]) or the mass extinction coefficients (c has the unit [mg/ml]).

3.6.10 ^{31}P NMR spectroscopy

Aliphatic, carboxylic, and phenolic hydroxyl groups were quantitatively determined with solution-state ^{31}P NMR spectroscopy (Granata and Argyropoulos, 1995). Lignin derivatized with 2-chloro-4,4,5,5-tetramethyl-1,3,2-dioxaphospholane (Aldrich) was analyzed in pyridine:deuterated chloroform solvent mixture containing chromium(III) acetylacetonate (Merck) as a relaxation agent, and endo-*N*-hydroxy-5-norbornene-2,3-dicarboximide (Sigma) as an IS. The spectra were recorded from 512 scans with 5 s relaxation time and 30° pulse angle using a Bruker Avance III 400 MHz spectrometer.

4 Results

The main objective of this work was to elucidate structural changes that occur in grass lignin during various treatments, and how they affect enzymatic digestibility of cellulose. The thesis publications **I**−**V** were undertaken in order to satisfy this objective. First, fractionation of maize stem lignin by sequential alkaline extractions was investigated (**I**). The second publication determined the effect of ball milling on maize stem lignin structure, and consequences on enzymatic digestibility of carbohydrates (**II**). Third, surface-accessible acidic hydroxyls of lignin were measured in solid-state using dye adsorption which provided method for determining lignin surface area (**III**). The fourth paper investigated changes in wheat straw lignin structure as a function of autohydrolysis severity and due to subsequent NH_3 (aq) extractions (**IV**). The straw solid residues generated in **IV** were subjected to enzymatic hydrolysis in order to elucidate the effect of modified lignin structure on enzymatic cellulose digestibility (**V**).

4.1 Effect of sequential extraction of maize stem on lignin structure[(I)]

In paper **I**, the sequential alkaline extractions of MS EFR were carried out at room temperature, and the structural components were characterized in the fractions. As was expected, the two extractions decreased the proportion of lignin and arabinoxylan in the solid residue fractions R1 and R3 (Table 4). The first extraction with 0.5 M NaOH removed 68% of lignin and 87% and 93% of the ester-linked FA and CA, respectively from MS EFR. The reduction in the content of etherified FA (77%) and CA (49%) from MS EFR to R1 was proportional to the removal of lignin, which is consistent with the fact that these phenolic acids are ether linked to lignin (Scalbert *et al.*, 1985). The UV-vis spectrophotometry showed that free FA and CA present in the first alkaline extraction liquid were not recovered in LC1 whose spectrum showed lower relative absorptivity in the wavelength region 320–360 nm (Fig. 14a), where the absorbance maxima of ionised FA ($\varepsilon_{346\ nm}$=23.7 mM^{-1} cm^{-1}) and CA ($\varepsilon_{333\ nm}$=23.9 mM^{-1} cm^{-1}) were observed (Fig. 14b).

Table 4. Composition and structural features of fractions obtained from maize stem extractive-free material (MS EFR) by sequential alkaline extractions and Novozyme 476 treatment according to the scheme shown in Fig. 12. This table summarizes data from Tables 1, 2, 4, and 5 in **I**.

Fraction[a]	Yield[b]	Klason lignin (KL)	Non-condensed lignin[c]	S/G ratio	Carbohydrates[d]		CA[e]		FA[f]	
					Glc	AX	ester	ether	ester	ether
	(%)	(% of DM)	(% of KL)		(% of DM)		(mg/g DM)		(mg/g DM)	
MS EFR	100	17.3	16.7	0.89	40.0	75.7	20.3‡	2.70‡	6.45‡	3.63‡
R1	(65.8)[g]	8.3	15.4	0.76	22.6	9.60	2.66	2.11‡	0.47‡	1.26
R2	(58.9)[h]	10.2	16.3‡	0.82	58.5	3.24	2.32	2.03	0.27‡	1.42‡
R3	42.3	7.7	11.5	0.61	19.6	47.0	0.32‡	1.94	0.06‡	1.37‡
LC1	17.4	38.3	23.4	1.21	59.5	2.66	7.28	8.23	1.71‡	12.3
LC2	7.62	18.7‡	2.0‡	1.06	20.7	63.2	0.31‡	2.80	0.03‡	2.73

[a]: R1–R3 stand for solid residues 1–3, and LC1 and LC2 are the fractions obtained after acidification of the alkaline extraction liquors 1 and 2. [b]: dry matter (DM) yield relative to MS EFR. [c]: calculated based on the yield of lignin monomers from thioacidolysis using 200 g/mol as the molecular weight of the lignin monomeric unit. [d]: Glc, glucan; AX, arabinoxylan; [e]: CA, *p*-coumaric acid; [f]: FA, ferulic acid; [g]: yield before Novozyme 476 treatment. [h]: yield before the second alkaline extraction. Results shown are mean values of duplicate determinations, with average deviation relative to the mean < 5%, unless marked with the ‡ symbol.

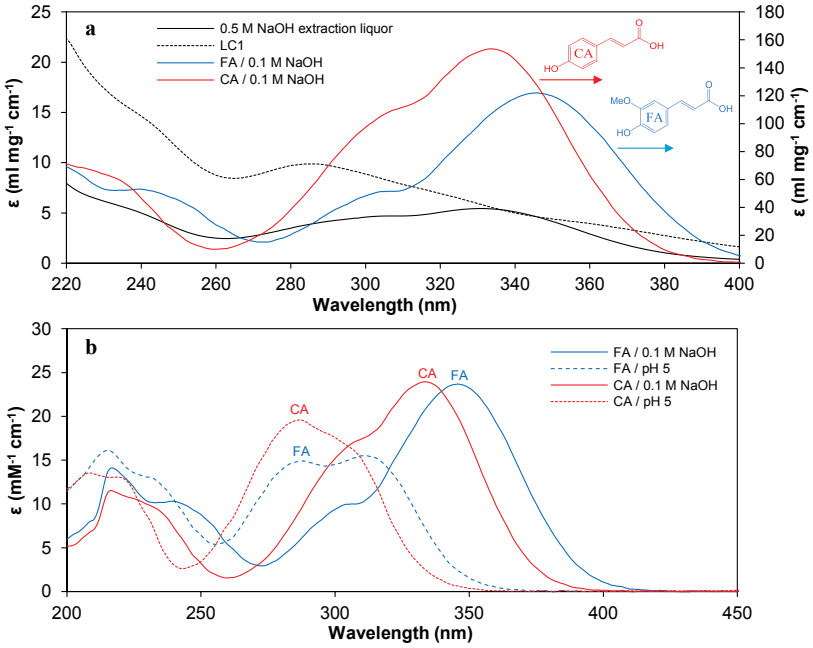

Figure 14. UV-vis spectra of **(a)** the first alkaline extraction liquid from MS EFR and LC1 fraction (in 0.2 M NaOH), in comparison to the spectra of ferulic acid (FA) and *p*-coumaric acid (CA) in 0.1 M NaOH; **(b)** CA and FA in 0.1 M NaOH (aq) and at pH 5 in 0.05 M Na-phosphate buffer (unpublished work).

Lignin structure in the fractions was analyzed by thioacidolysis which generates trithioethylated monomers from non-condensed lignin units which are only linked by β-O-4 bonds (Rolando *et al.*, 1992). The thioacidolysis products were separated using GC and detected based on their known mass fragments. This was a powerful technique because specific m/z values could be used to reconstruct chromatograms with improved resolution of the lignin-derived monomers (Fig. 15). Thioacidolysis results showed that lignin in LC1 contained 23% of non-condensed units which is 40% more than in the starting material (Table 4). This first LC fraction probably originated from the ML and CC regions which contain the highest proportion of easily extractable lignin in grasses. Another detected difference was the higher relative proportion of **S** units in LC1 (**S**/**G**=1.21) as compared to the starting material MS EFR (**S**/**G**=0.89). This was consistent with the earlier results with wheat straw (Fidalgo *et al.*, 1993), and in agreement with the higher proportion of non-condensed linkages in LC1.

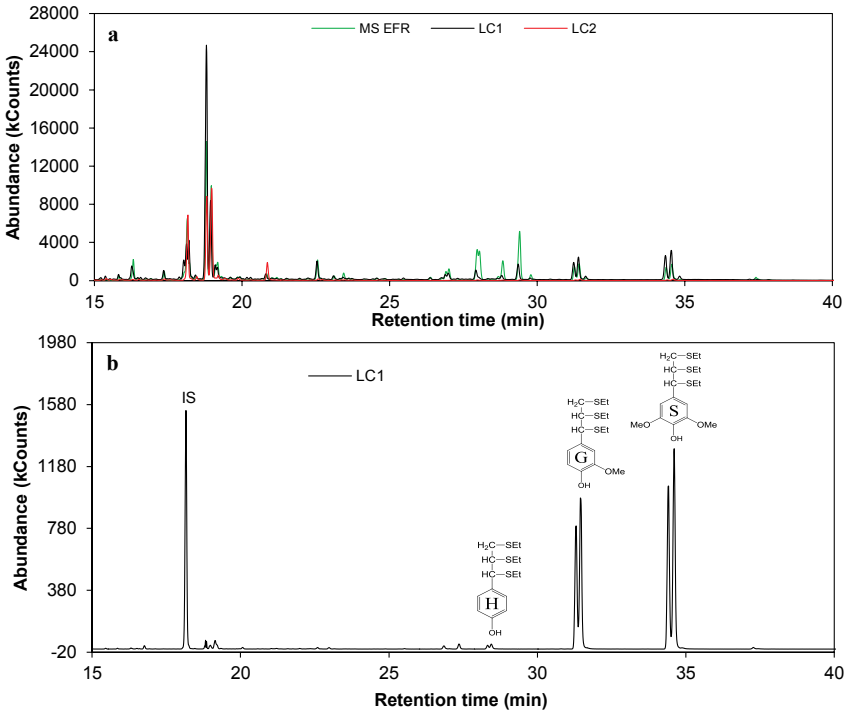

Figure 15. Partial GC/MS traces of lignin-derived thioacidolysis products: **(a)** total ion count of MS EFR, LC1, and LC2; **(b)** Reconstructed ion trace of LC1 using m/z values 57+71+85 (heneicosane as IS), 239 (**H**), 269 (**G**), and 299 (**S**). These chromatograms were used to determine lignin structure in **I**, but the figures have not been previously published.

Hydrolytic treatment with Novozyme 476 made it possible to isolate lignin from the partially cleaved cell walls. In turn, substantially different lignin was detected in LC2 which contained only 2% of non-condensed lignin. In

summary, two distinct alkali-soluble fractions containing contrastive lignin structures were obtained from the sequential extraction procedure. Adding to the earlier knowledge (Crestini *et al.*, 2011), the results of the current thesis suggest that the less branched lignin in the easily extractable fraction could be a general feature shared by wood and grass lignocellulose. Within the latter group, the existence of two distinct lignin fractions were also suggested after alkaline extraction of sugarcane bagasse based on fluorescence microscopy (Coletta *et al.*, 2013). Beyond this qualitative information, one valuable aspect of the current thesis is that it provided unambiguous quantitative results of the fractionation of lignin structure at the molecular level.

4.2 Effect of ball milling on maize stem lignin structure and on enzymatic carbohydrate hydrolysis[(II)]

Ball milling is an efficient laboratory technique for increasing solubility of lignocellulosic materials for subsequent liquid-state analysis or extraction (Lu and Ralph, 2003; Balakshin *et al.*, 2011). The publication **II** investigated the effect of ball milling of maize stem on the structure of lignin and further on enzymatic hydrolysis of carbohydrates. The lignin aryl ether linkages were determined by thioacidolysis which showed decreasing total yield of **H**, **G**, and **S** monomers as a function of milling time (Fig. 16). However, when the analysis was conducted after the milled materials were treated with the hydrolytic enzyme Onozuka R-10, the thioacidolysis yields from the solid residues were similar as obtained from the MS EFR without milling. Therefore, it was confirmed that aryl ether linkages were not cleaved, but instead the high intensity ball milling rendered the grass material resistant towards chemical depolymerization of lignin. These results should turn out highly useful for interpretation of data from various analytical methods based on ball milling.

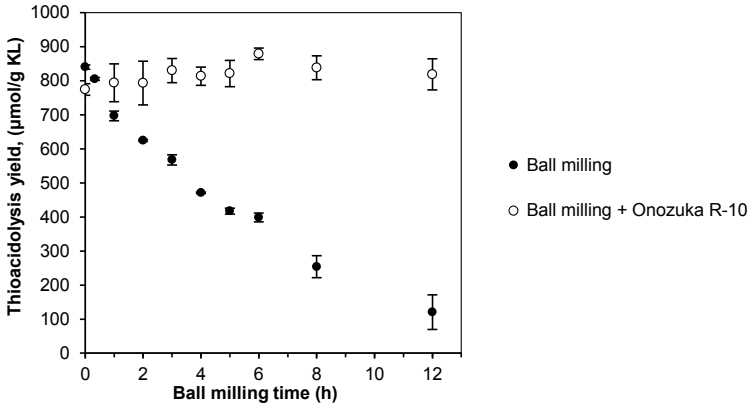

Figure 16. The effect of ball milling time on total yield of *p*-hydroxyphenyl (**H**), guaiacyl (**G**), and syringyl (**S**) lignin monomers from thioacidolysis of ball-milled maize stem material or solid residues obtained after Onozuka R-10 treatment of the milled materials (reproduced from Fig. 4 in **II**).

A closer look into the thioacidolysis products obtained as a function of ball milling time revealed differences in their molar mass distributions compared to the products from the starting material MS EFR without milling (Fig. 17). The signal intensity in the oligomeric region at retention times 12–16 min increased as a function of increasing amount of lignin in the thioacidolysis reaction due to the prior removal of carbohydrates. Furthermore, the relative intensity of the two distinct peaks in the monomer region at retention times 16–17 min changed as a consequence of the Onozuka R-10 treatment conducted before thioacidolysis. Spectrophotometric analysis of the liquid fractions obtained by extraction of the milled materials suggested that FA and CA were removed from the solid materials with the hemicellulose fragments (Fig. 2 in **II**).

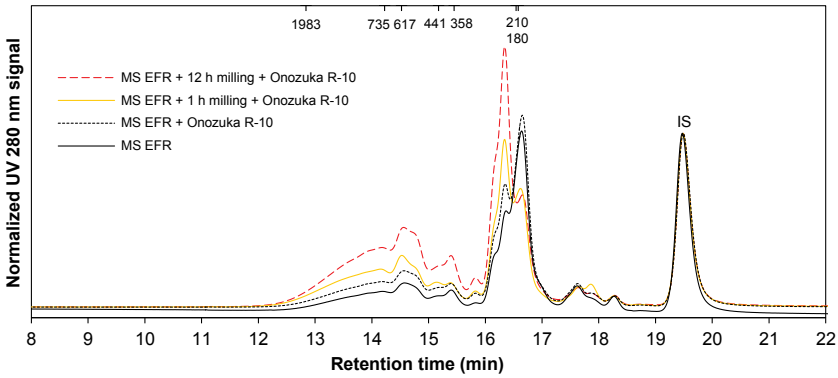

Figure 17. HPSEC chromatograms of thioacidolysis products from maize stem extractive free residues (MS EFR) or from solid residues of MS EFR or ball-milled MS EFR after treatment with Onozuka R-10 at 45 °C for 72 h. Chromatograms were normalized relative to the IS signal of 2,3-dimethoxytoluene. Molecular weight standards (1983–180 g/mol) are indicated at their corresponding retention times (unpublished work).

In contrast to the moderate changes found in lignin structure, maize stem hemicelluloses were extensively depolymerized as indicated by the increasing amounts of monosaccharides released in the aqueous extraction of the solid materials as a function of increasing milling time (Fig. 2 in **II**). Carbohydrate conversion from the 72 h enzymatic reaction of ball-milled materials catalyzed by Onozuka R-10 increased with increasing milling time up to 4 h, but did not increase further thereafter (Fig. 18). Hydrolysis of up to 92% of cellulose suggested that the presence of lignin does not alone impede efficient hydrolysis of cellulose when LCN was partially depolymerized, and the relative crystallinity of cellulose was below 28% of the original level. In contrast to cellulose, arabinoxylan resisted enzymatic hydrolysis regardless of the milling time, suggesting that lignin and LC linkages remained as the major structural constraints (Fig. 18). Consequently, total carbohydrate conversion from the milled materials did not exceed 80%.

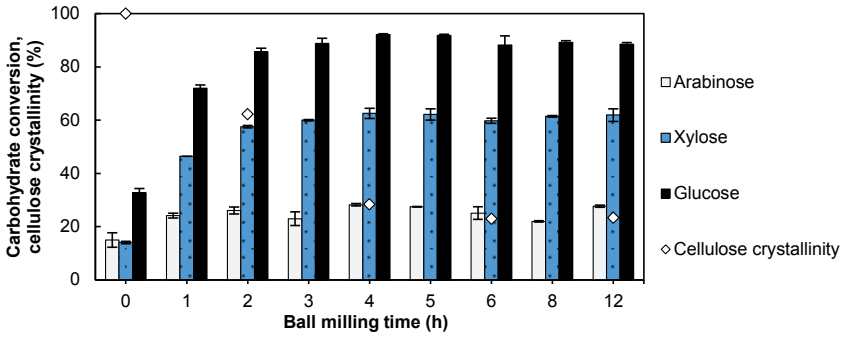

Figure 18. The effect of ball milling time on relative cellulose crystallinity and subsequent carbohydrate conversion of ball-milled maize stem materials after treatment with Onozuka R-10. The errorbars represent average deviation from the mean values of duplicate experiments (reproduced from data in Table 1 and in Fig. 3 in **II**).

The effect of hemicellulose-associated lignin on enzymatic digestibility of carbohydrates was studied further using LC1 and LC2 from **I** as model materials, as these fractions did not contain crystalline cellulose which is itself a recalcitrant substrate for cellulases. It was found that carbohydrates of LC2 were fully hydrolysed, whereas 17% of carbohydrates in LC1 resisted enzymatic hydrolysis (Table 2 in **II**). The higher alkalinity used in the isolation of LC2 removed almost completely the ester linked CA and FA that were still present in LC1, and known to be involved in LC interlinkages (Iiyama *et al.*, 1994). Put together, these results showed that LC-linkages impede enzymatic hydrolysis of carbohydrates. The chemical and mechanical treatments of maize stem in **I** and **II** were carried out at room temperature. It is notable that more extensive changes in lignin structure are expected to occur during industrial pretreatment processes which are carried out at elevated temperatures. Thus, direct *in planta* characterization of lignin in solid-state is a necessity for obtaining more utilisable information of the changes in lignin structure during pretreatment.

4.3 Development of a quantitative method for characterization of lignin surface area by Azure B adsorption[(III)]

In addition of gaining information of chemical changes of lignin in various chemical and mechanical treatments, lignin was suspected to undergo morphological property changes during pretreatment of lignocellulose. It is known that incorporation of grass lignin onto cellulosic fibers increases their water resistance (Sipponen *et al.*, 2010), which is a potentially detrimental feature for enzymatic hydrolysis of carbohydrates that necessitates interaction between water-soluble enzymes and insoluble surfaces. This background together with the information gained from **I** and **II** led to a hypothesis that morphology of lignin in solid fractions is in a key role in enzymatic hydrolysis

of cellulose. Therefore, a target was set to develop a new method for determination of lignin surface area in solid-state at neutral pH. Cationic dye Azure B is available as a synthetic reagent, and it contains a central heteroatom ring with basic nitrogen (Fig. 19). These traits were considered to be well-suited for probing lignin whose phenolic hydroxyl groups are weakly acidic.

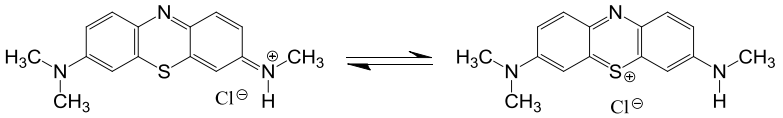

Figure 19. Molecular structure of the Azure B showing delocalization of the cationic charge.

The effect of pH on adsorption of Azure B on lignocellulosic materials was first investigated. Adsorption of Azure B on wheat straw and on GreenValue lignin (from industrial soda pulping of wheat straw) showed increased equilibrium adsorption capacity (q_e) when pH increased from pH 3 to pH 6–7 (Fig. 20). In contrast, the low level of adsorption of Azure B on cellulose was not affected by pH. Acetylated GreenValue lignin showed similarly low q_e as cellulose until pH 6, and further increase to pH 8 showed only a slight increase in its q_e. These initial results suggested rather specific binding of Azure B on phenolic hydroxyl groups because acetylation did not block the carboxylic hydroxyl groups of lignin (Table 2 in **III**). The proposed binding mechanism thus involves deprotonation of lignin's phenolic hydroxyl group by the nitrogen in the heteroatom ring of Azure B, leading to simultaneous ionic bond formation.

The adsorption kinetics was investigated using WS as adsorbent, and in order to assess selectivity of the dye binding on the available surfaces. With each of the initial concentrations of Azure B, adsorption proceeded rapidly within the first 2 h and thereafter began to slowly reach a plateau (Fig. 21a). The kinetic data were assessed further according to a model which assumes that adsorption in a system limited by intra-particle diffusion gives a linear relation between q_e and $t^{0.5}$ (Allen *et al.*, 1989). The Azure B adsorption revealed multi-linearity, which indicates dynamic stepwise changes in the adsorption process, a trend also observed by Sun and Yang (2003) with peat particles. In contrast to the earlier results with peat, in the current work WS gave almost similar kinetic parameters for the first adsorption stage ($k_{i,1}$), regardless of the initial concentration of Azure B (Fig. 21b). Thus, intra-particle diffusion did not limit adsorption of the dye on the readily accessible acidic hydroxyl groups, arising from the prevalent porous hollow structures in WS. The kinetic data therefore supported the application of the Azure B to the surface characterization.

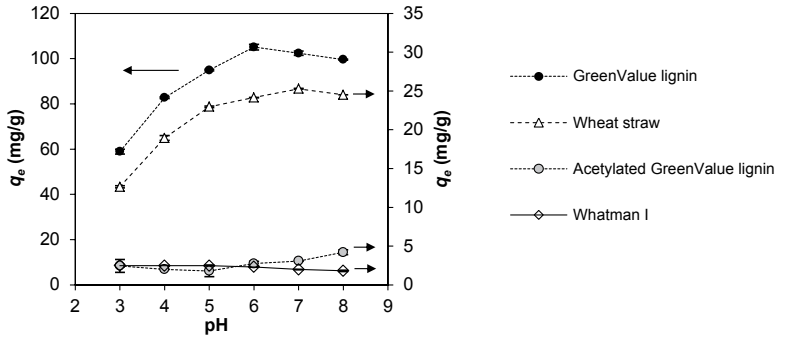

Figure 20. The effect of pH on adsorption of Azure B on GreenValue lignin, wheat straw, acetylated GreenValue lignin, and Whatman I cellulose fibers. Equilibrium adsorption capacity (q_e) is shown from experiments with 24 h contact time at 25 °C. Each series was carried out using 0.1 g/l Azure B in pH buffer solution and constant amount of the adsorbent: lignin materials (50 mg lignin in 50 ml), WS and Whatman I (100 mg in 25 ml). The errorbars represent average deviations from the mean values of duplicate experiments (**III**).

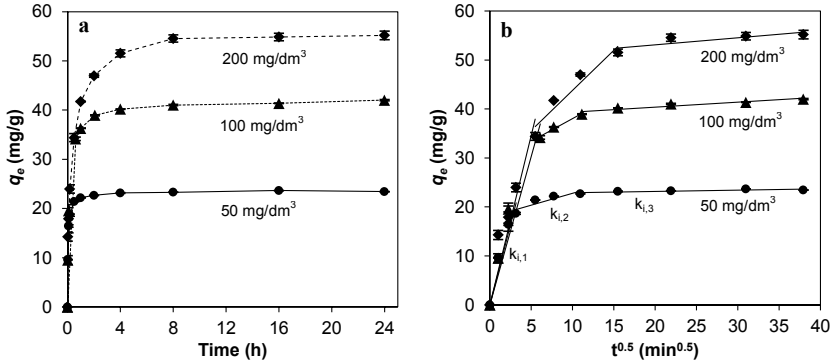

Figure 21. Time-course of adsorption of Azure B on wheat straw: **(a)** equilibrium adsorption capacity (q_e) as a function of contact time at 50−200 mg/dm^3 initial Azure B concentrations; **(b)** intraparticle diffusion model showing the kinetic constants (the slopes of the lines whose units are mg/g/min$^{0.5}$) $k_{i,1}$=6.59, $k_{i,2}$=0.48, $k_{i,3}$=0.03 (50 mg/dm^3), $k_{i,1}$=6.07, $k_{i,2}$=0.92, $k_{i,3}$=0.10 (100 mg/dm^3), $k_{i,1}$=6.92, $k_{i,2}$=1.64, $k_{i,3}$=0.14 (200 mg/dm^3). The errorbars represent average deviation from the mean values calculated from the results of duplicate experiments (**III** and unpublished work).

Maximum equilibrium adsorption capacities (X_m) were determined from the Langmuir isotherms fitted for WS, SGB, oat husk, and the two wheat straw lignin and cellulose reference materials at pH 7 (Fig. 22). The two lignin materials showed 5−13-fold higher X_m values than those of the crop residues, whereas the cellulose materials showed low X_m levels, confirming that Azure B did not preferentially adsorb on non-charged carbohydrates (Table 5). Grass hemicellulose contains 4-*O*-methylglucuronic acid moieties bearing free carboxylic groups. Pectin is another possible source of acidic groups, although a majority of the galacturonic acid residues are methyl esterified in the primary

cell walls, and altogether pectin is a minor component amounting 0.5% of the WS dry weight (Sun *et al.*, 1998). Although adsorption of Azure B on the acidic carbohydrate residues might occur, the possible interference was expected to be low since uronic acids comprise only approximately 1% of WS dry weight (Holopainen-Mantila *et al.*, 2013). Furthermore, it is evident from Fig. 22 that lignin is the main component responsible for the dye binding. It should be also noted that the lignocellulose materials gave zero absorbance at 647 nm, and also the lignin materials led to negligible absorbances below 0.15, when incubated in buffer solution without Azure B.

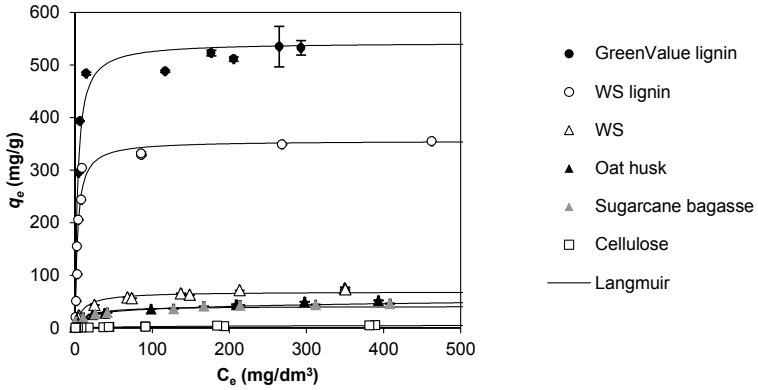

Figure 22. Adsorption of Azure B on lignocellulosic materials. Continuous lines represent Langmuir isotherms fitted to the equilibrium adsorption data. Errorbars represent average deviations from the mean values calculated from duplicate experiments (reproduced from **III**).

The X_m values obtained from the Langmuir isotherms were used to calculate the amount of surface-accessible acidic hydroxyls and lignin surface area (SA). Among the crop residues WS showed the highest lignin SA (84 m^2/g), followed by SGB (53 m^2/g) and oat husk (48 m^2/g) materials (Table 5). WS lignin and GreenValue lignin had 5− and 15−fold higher lignin SA compared to those of the crop residues. In order to assess these results quantitatively, the contents of surface-accessible acidic OH groups in the lignin materials were compared to the total amounts of acidic OH groups as determined by solution-state ^{31}P NMR. WS lignin and GreenValue lignin contained 3.13 mmol/g and 3.73 mmol/g acidic hydroxyls, which were, respectively, 2.7− and 2.1−fold higher than those determined by the adsorption method. On this basis, the dye adsorption appeared to give consistent results because solid-state morphology limits access to the adsorption sites. The curiously different proportions of surface-accessible acidic hydroxyls found in the two wheat straw alkali lignin materials urged further structural investigation. These experiments were planned to reveal the effect of lignin structure on the proportion of surface-accessible acidic hydroxyl groups in solid state.

Table 5. Maximum equilibrium adsorption capacities (X_m), surface-accessible acidic hydroxyls and lignin surface area (SA) of lignocellulose materials. The R^2 values are from the fit of experimental data to the Langmuir model (Eq. 1) (**III**).

Material	R^2	X_m [a] (mg/g material)	X'_m (mg/g lignin)	Surface-accessible	
				Acidic OH[b] (mmol/g material)	Lignin SA[c] (m^2/g material)
Wheat straw	0.991	68.9 ± 0.3	291	0.21	84
SGB[d]	0.923	45.5 ± 0.6	191	0.13	53
Oat husks	0.958	41.2 ± 1.0	181	0.12	48
WS lignin	0.972	356 ± 2	429	1.16	460
GreenValue lignin	0.899	543 ± 2	593	1.77	703
Whatman I	0.973	1.65 ± 0.3	-	-	-
Emcocel 50M	0.943	5.63 ± 0.3	-	-	-

[a]: The value after ± indicates standard deviation from the mean value, calculated from the results of duplicate experiments. [b]: Calculated from Eq. 2. [c]: Calculated from Eq. 3. [d]: SGB, sugarcane bagasse.

4.4 Structural assessment of two wheat straw alkali lignins

The properties of lignin depend on the type of lignocellulose and the isolation process used. GreenValue lignin and WS lignin differed remarkably in their surface areas as determined with Azure B adsorption. Both of the materials were obtained from soda cooking of wheat straw either from an industrial process (GreenValue lignin) or from a bench-scale process comprising 5 h autohydrolysis at 140 °C, NaOH cooking of the solid fraction at similar conditions, followed by precipitation and purification at pH 5. Elemental analysis showed the following weight proportions: 63.8% C, 6.1% H, 1.0% N in GreenValue lignin and 58.6% C, 5.3% H, 0.6% N in WS lignin, values consistent with their lignin contents (Table 2). However, even when calculated relative to the total lignin content, higher proportion of surface-accessible acidic hydroxyl groups was found in GreenValue lignin (Table 5).

Comparison of the ^{31}P NMR spectra of the two lignin materials revealed some clear differences (Fig. 23a). First, WS lignin showed a distinct peak at 136.7 ppm, not present in the spectra of GreenValue lignin, but occasionally detected in the ^{31}P NMR spectra of straw lignin (Argyropoulos, 2014). Recent evidence suggests that the flavonoid tricin is linked to wheat straw lignin via ether linkage (del Río *et al.*, 2012), and that the C7-*O* signal of free tricin occurs at 136.4 ppm (Heikkinen *et al.*, 2014). Therefore, it is possible that the 136.7 ppm signal stems from flavonoids, tannins, or other related substance incorporated into straw lignin, but degraded during a more severe industrial NaOH cooking that generated GreenValue lignin. This would be in accordance with the presence of 28% more carboxyl groups in GreenValue lignin compared to WS lignin (Fig. 23a). These differences may also arise from botanical variations as GreenValue lignin contained nearly three times more phenolic *p*-hydroxyphenyl units compared to WS lignin (Fig. 23b).

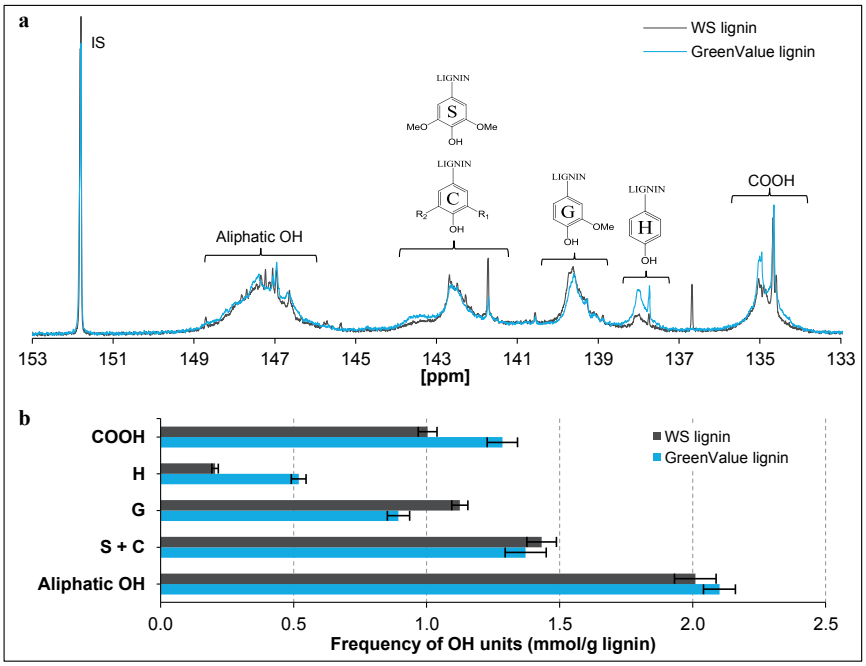

Figure 23. Hydroxyl group analysis of WS lignin and GreenValue lignin: **(a)** assignment of the ^{31}P NMR spectra; **(b)** Distribution of hydroxyl groups: COOH, carboxylic OH; **H**, **G**, and **S** refer to the phenolic OH in the corresponding units. **C** refers to the phenolic OH in condensed aromatic rings (Granata and Argyropoulos, 1995). R_1=H, C, OMe, and R_2=C. Neutral carbohydrate residues detected after acid hydrolysis (Table 2) contribute slightly to the aliphatic hydroxyls (WS lignin, 0.02 mmol/g; GreenValue lignin, 0.07 mmol/g). Errorbars represent average deviations from the mean values of triplicate experiments (unpublished work).

Lignin structure was assessed further through analysis of phenolic products from the alkaline CuO oxidation of the two lignin materials. According to the previously unpublished results, WS lignin and GreenValue lignin showed similar total yields of the nine identified monophenols (79 ± 3 mg/g lignin), but contrastive **S**/**G** ratios. WS lignin (**S**/**G**=0.65 ± 0.07) contained lower relative proportion of **S** units compared to GreenValue lignin (**S**/**G**=0.97 ± 0.08) even though no major differences were observed in the relative proportions of free **S** and **G** type phenolic groups (Fig. 23b). It can be speculated that the lower **S**/**G** ratio of WS lignin resulted from the removal of lignin **S** units either in the autohydrolysis or the xylanase treatment conducted before and after the NaOH delignification, respectively.

No major qualitative differences were observed in the UV-vis spectra of the two lignin materials. When calculated relative to the total lignin content of the material, WS lignin showed slightly higher absorbance than GreenValue lignin, with maxima at 219 nm, minima at 284 nm (ε=27.8 ml/(mg lignin·cm) and ε=25.8 ml/(mg lignin·cm), respectively) and shoulders approximately at 250 nm and 350 nm (Fig. 24a). Furthermore, molar mass distributions showed

identical polydispersities of 3.3 and almost similar $\bar{M}_w$ of WS lignin (3260 g/mol) and GreenValue lignin (2820 g/mol) (Fig. 24b).

Since various solution-state analyses suggested more structural similarities rather than discrepancies between the two lignin materials a hypothesis was proposed that the main difference between the materials arose from their solid-state morphologies. Accordingly, WS lignin adopted more closed particle structure than GreenValue lignin. This might be a result of the autohydrolysis (140 °C, 5 h) carried out prior to solubilization of WS lignin. A systematic investigation was thus carried out as an attempt to elucidate the impact of autohydrolysis severity on lignin structure.

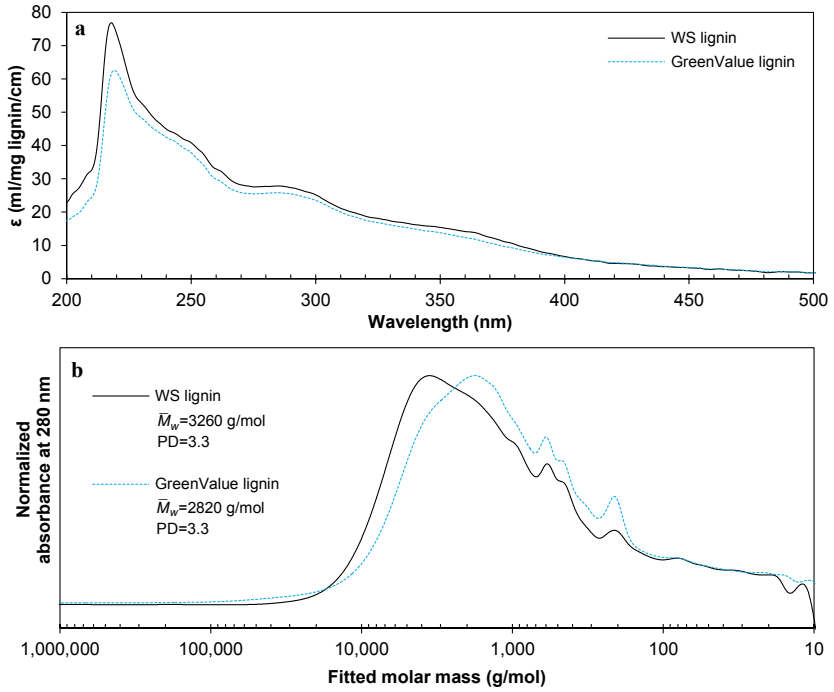

Figure 24. Comparison of WS lignin and GreenValue lignin on the basis of: **(a)** UV-vis spectra recorded in 0.1 M NaOH and expressed as absorbance per dry weight of lignin in solution; **(b)** Normalized molar mass distribution based on the HPSEC chromatograms showing VWD signal at 280 nm. The fitted molar mass was calculated based on the relative calibration (R^2=0.994) (unpublished work).

4.5 Effect of autohydrolysis and aqueous ammonia extraction on wheat straw lignin[IV–V]

Surface elemental composition of WS milled to pass a 0.2 mm sieve was determined by EDS which showed signals for Si, K, and Ca, in addition to the predominant C and O signals (Fig. 25a). In contrast, Si was the main inorganic element on the external straw surface in the EDS spectrum (Fig. 25b) recorded at the rectangular area visualized in the SEM micrograph (Fig. 25c). For comparison, inner microstructure of WS milled to pass a 1-mm sieve is shown in Fig. 25d. This batch of WS comprising 39% cellulose, 26% hemicelluloses, 1.9% acetyls, 21.8% Klason lignin, 3.1% protein, 0.4% esterified FA and CA, and 4.2% ash was subjected to AH and subsequent alkaline extractions. These experiments were planned to elucidate the structural changes in lignin as a function of pretreatment severity and consequential effects on subsequent enzymatic hydrolysis of cellulose.

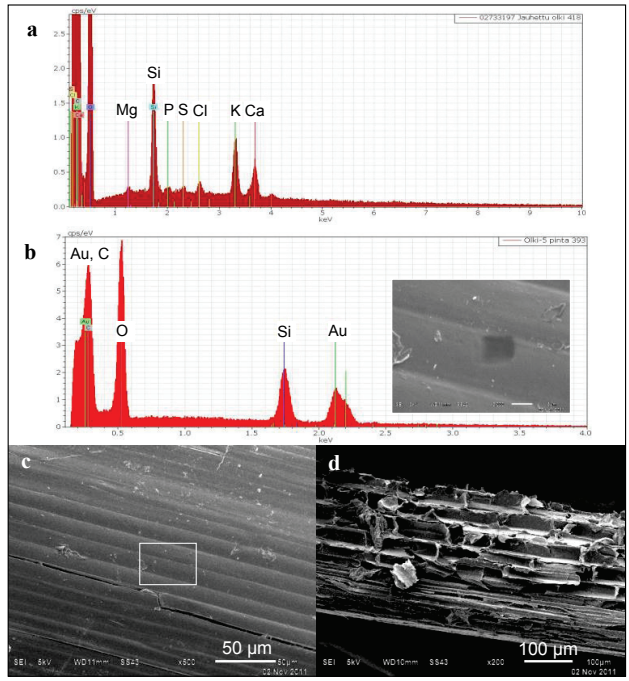

Figure 25. Surface characterization and visualization of wheat straw: **(a)** elemental analysis by energy dispersive spectroscopy (EDS) of straw milled to pass a 0.2 mm sieve; **(b)** external straw surface showing the predominant Si signal, and the Au signal from the coating conducted in order to capture the SEM micrographs of **(c)** external surface of straw milled to pass a 1 mm sieve, with the rectangular area showing the area investigated by EDS; **(d)** straw interior (unpublished work).

Fractionation of lignin between the solid and liquid phases was followed from the mass balances of the treatments. In AH, the percentage dissolution of lignin increased from 10% to 20% when severity (Log R_0) increased from 3.1

to 3.5, respectively, and thereafter remained between 14% and 24% (Fig. 26). These results suggest that wheat straw contained a lignin fraction that was readily dissolved at low severity. Alternatively, simultaneously occurring precipitation would explain the asymptotic lignin dissolution. The water-soluble total phenolics determined as gallic acid equivalents (GAEs) using the Folin-Ciocalteu reagent showed only a weak positive linear correlation with percentage dissolution of lignin (R^2=0.43). Therefore, water-soluble lignin did not contain a high proportion of free phenolic hydroxyls. Monomeric phenolic compounds were analyzed in the AH liquors also with HPLC in order to investigate the possible origin of the phenolic compounds. Among the identified lignin-derived compounds only vanillin gave positive correlation with increasing AH severity (R^2=0.93), whereas the concentrations of monomeric (HPLC) and total (GAEs) phenolic compounds did not correlate. Furthermore, dissolution of arabinoxylan and lignin showed only a weak correlation (R^2=0.40). To summarize, these results suggest that lignin dissolved mainly as oligomeric or polymeric fragments during AH, independent of arabinoxylan dissolution.

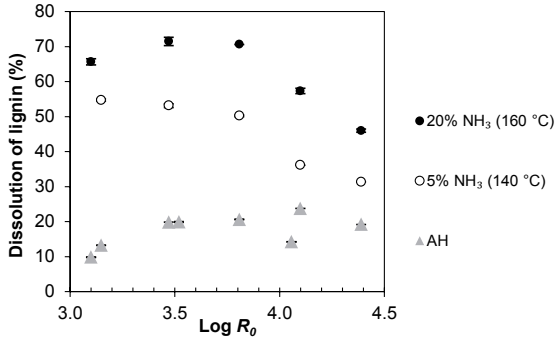

Figure 26. Dissolution of lignin from wheat straw solid fractions as a function autohydrolysis (AH) severity (Log R_0): after AH (triangles) and after successive extractions of the AH solid residues with 5% NH_3 at 140 °C (white circles) or with 20% NH_3 at 160 °C (black circles). Errorbars represent average deviations calculated from duplicate composition analysis results (Based on data in Table 2 and Fig. 5 in **IV** and Table 1 in **V**).

In the extraction step, percentage dissolution of lignin from AH solid residues was dependent on the preceding AH severity and intensity of the alkaline extraction (Fig. 26). The high intensity extraction solubilized up to 72% of lignin at AH severity of 3.5, whereas the dissolution in the moderate intensity extraction decreased from 55% to 31% as AH severity increased. In both cases, a threshold was observed at severity of 3.8 after which the dissolution of lignin dropped rapidly with increasing severity. Reduced extractability of AH solid residues of wood has previously been attributed to so-called re-polymerization reactions of lignin involving a carbocation intermediate and occurring in parallel with depolymerization (Wayman and Lora, 1978; Li *et al.*, 2007).

However, it should be noted that in the current work the threshold was found in the same point at which drastic hemicellulose degradation commenced as evidenced by increasing concentrations of furfural detected in the AH liquors (Table 2 in **IV**). Furfural was recently suggested to undergo acid-catalyzed Diels-Alder homopolymerization in aqueous medium (Danon *et al.*, 2013). Instead of the Diels-Alder reaction between furfural and lignin which would unfavorably deplete the aromatic electron system in lignin, furfural or its polymerization products might react with the lignin carbocation formed in the solid fraction. Although identification of these structures was not attempted in the current work, the presence of such cross-linked lignin structures would explain the observed resistance of wheat straw solid residues to alkaline extraction after high AH severities (Fig. 26).

The soluble materials released during NH_3 (aq) extractions of the AH solid residues were analyzed for $\bar{M}_w$ of lignin using HPSEC. The decreasing $\bar{M}_w$ as a function of severity (Fig. 27a) correlated with carbohydrate content of the extract (R^2=0.93), also decreasing with increasing severity (Fig. 27b). This trend suggested that deconstruction of LCN occurred during AH as a result of hydrolysis of hemicelluloses. As judged from the difference between the $\bar{M}_w$ values resulting from the two extraction intensities, the high intensity extraction depolymerized LCN further until severity of approximately 4.0, presumably by cleavage of residual LC-linkages and aryl ether linkages of lignin. Thereafter, further increase in AH severity did not change $\bar{M}_w$ of lignin.

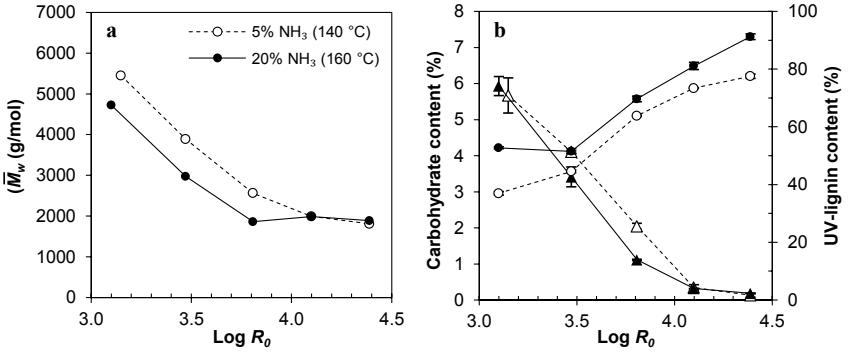

Figure 27. The effect of wheat straw autohydrolysis (AH) severity (Log R_0) on aqueous ammonia extracts obtained at 140 °C (5% NH_3, white markers) or at 160 °C (20% NH_3, black markers) from the AH solid residues: **(a)** weight average molar mass ($\bar{M}_w$) (single determinations); **(b)** content of carbohydrate (triangles) or UV-lignin (circles). Errorbars represent average deviations from the mean values calculated from duplicate experiments (**IV**).

Altered lignin structure was found in the alkali-soluble materials isolated by extraction of the AH solid residues with 5% NH_3 (140 °C) (Fig. 7 in **IV**). The yield of phenolic compounds from the CuO oxidation of the aqueous ammonia extracts decreased as much as 55% as a function of AH severity, suggesting reduction in the proportion of native lignin either due to cleavage of aryl ether bonds or accumulation of alkali-soluble material termed pseudo-lignin. These results were obtained from isolated materials whose lignin content was based on the UV absorbance which is affected by the molar mass distribution and possible presence of degradation products. To rule out any interference from lignin fractionation and in order to elucidate the effect of pretreatment on lignin structure the solid residues obtained from AH alone or AH with subsequent NH_3 (aq) extractions were subjected to CuO oxidation.

The results shown in Fig. 28a confirmed degradation of lignin originally present in WS, since as much as 39% lower yield of CuO oxidation products was obtained from the AH solid residues. The high intensity NH_3 (aq) extraction of the AH solid residues decreased the yield of phenolic oxidation products further by 34−48%. Effectively, the yield of CuO oxidation products from the double treatment (AH+extraction) at the highest severity was 61% lower than the yield from untreated WS (168 mg/g lignin). Similar change was not obtained with the extraction at the lower intensity (5% NH_3, 140 °C), although then less lignin dissolved (Fig. 26). These results suggested that alkaline cleavage of lignin occurred readily only at the high intensity extraction, where alkalinity (final pH 12) and temperature (160 °C) were comparable and pressure (16 bar) exceeded those of industrial alkaline pulping processes. Lignin **S/G** ratios were determined from the detected syringyl and guaiacyl type CuO oxidation products. Statistically insignificant changes in the **S/G** ratios were found after AH, but in contrast the NH_3 (aq) extractions decreased the **S/G** ratios in the final solid residues compared to those of the AH solid residues Fig. 28b. This was consistent with the reduction of lignin **S/G** ratios in solid residues after extraction of maize stem (**I**) or WS with NaOH (Fidalgo *et al.*, 1993). To sum up, alkaline extraction mainly solubilized and cleaved lignin enriched in **S** units which were involved in aryl ether linkages. The methoxyl group at the C5 position in lignin **S** units was a likely molecular level reason for this selective fractionation.

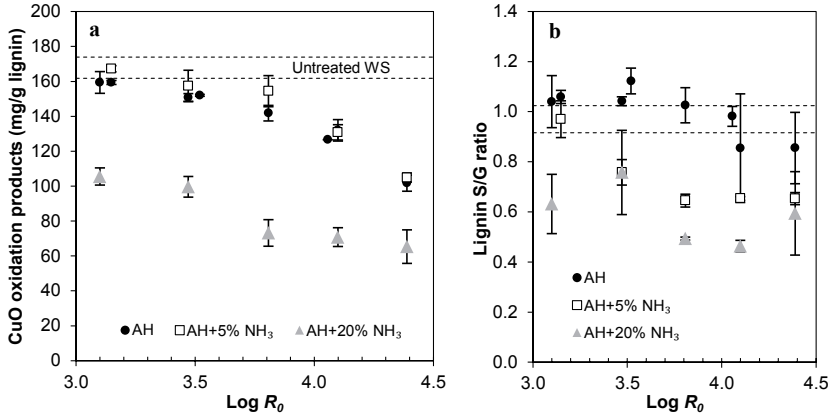

Figure 28. The effect of wheat straw autohydrolysis (AH) severity (Log R_0) on **(a)** total yield CuO oxidation products released from solid residues obtained after AH (black circles) or after subsequent extraction with 5% NH_3 (aq) at 140 °C (squares) or with 20% NH_3 (aq) at 160 °C (triangles) **(b)** Lignin **S**/**G** ratios calculated from the identified phenolic oxidation products: **S**=acetosyringone+syringaldehyde+syringic acid; **G**=acetoguaiacone+vanillin+vanillic acid. Errorbars represent average deviations from the mean values calculated from duplicate experiments. The dashed lines indicate mean values of untreated WS ± average deviation (unpublished work).

Severity is one of the key pretreatment parameters as it governs the impacts on the lignocellulosic feedstock. The central results of **IV** and **V** regarding deconstruction of WS during AH were summarized as a function of severity in Fig. 29. The yield of solid residues first decreased rapidly due to the release of hemicelluloses and other water-soluble substances. The yield of hemicelluloses in the liquid phase first increased with increasing severity, but decreased after the maximum yield due to drastic sugar degradation after severity of 4. When most of the hemicelluloses were released at severities over 4, the yield of solid residues did not further decrease below 67%. Enzymatic digestibility of cellulose increased non-linearly and the yield of native lignin decreased linearly in the severity region of this work (3.1−4.4). The maximum sugar yield from the overall process comprising AH at severities between 3.8−4.1 and subsequent 24 h enzymatic hydrolysis reactions was 73−74% when calculated relative to the carbohydrates in untreated WS. It is noteworthy that in this severity region where the maximum sugar yield was obtained approximately 40% of “native” lignin had been lost from the solid residues (Fig. 29).

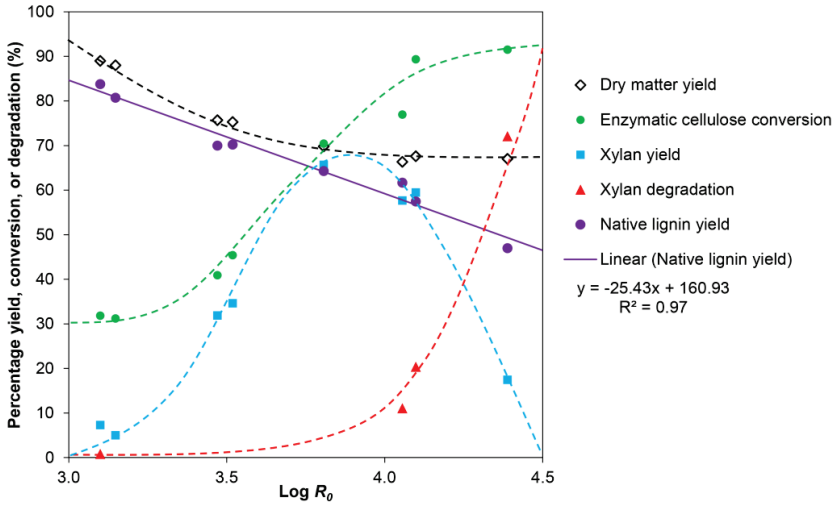

Figure 29. The effect of autohydrolysis severity (Log R_0) on wheat straw and its main components. The dashed lines illustrate trends of the experimental data calculated on dry weight basis. Xylan yield = 100% · g xylose in liquid phase/g xylose in wheat straw feed. Xylan degradation = 100% · [(g xylose in WS-xylose in liquid phase-g xylose in solid residues)/g xylose in WS]. Enzymatic cellulose conversion = 100% · (g glucose · 0.90/g cellulose in AH solid residues), after 24 h reaction catalyzed by 15 FPU/g cellulase activity. Native lignin yield = 100% · [g CuO oxidation products from AH solid residues·DM yield]/[g CuO oxidation products from WS]) (**IV**−**V** and unpublished work).

The effect of AH severity on lignin SA was a key novel finding revealed using the developed dye adsorption method. Lignin SA decreased from 84 m^2/g in untreated WS to 47 m^2/g in the solid residues obtained at the highest AH severity (Fig. 30a). In parallel, 20% dissolution (Fig. 26) and 39% cleavage of lignin occurred (Fig. 28a). Interestingly, when lignin SA was divided with lignin content of the material, the obtained lignin SSA showed linear correlation with severity (Fig. 30b). As opposed to the contrastive effects of the moderate and high intensity NH_3 (aq) extractions on chemical structure of lignin, both of the two extractions increased lignin SSA from the AH solid residues. Possible effect of structural fractionation on lignin SSA could be ruled out because extraction with 5% NH_3 at 140 °C did not change lignin structure in the solid residues (Fig. 28a). Moreover, alkali-solubility of grass lignin arises from its frequent phenolic hydroxyl groups (Lapierre *et al.*, 1989), and the alkaline extractions carried out after AH might have instead enriched non-phenolic lignin in the solid residues. The latter speculation could be refuted simply because the quantification of lignin SA was based on the determination of acidic OH groups of lignin among which phenolic hydroxyls are the most prominent ones. The observed changes in lignin SA and SSA were thus concluded to be arising from morphological changes in lignin. Inaccessible lignin was formed as a result of densification of lignin during AH,

whereas the alkaline extractions of the AH solid residues led to incomplete dissolution of the aggregated lignin which enriched onto surfaces of the final solid residues.

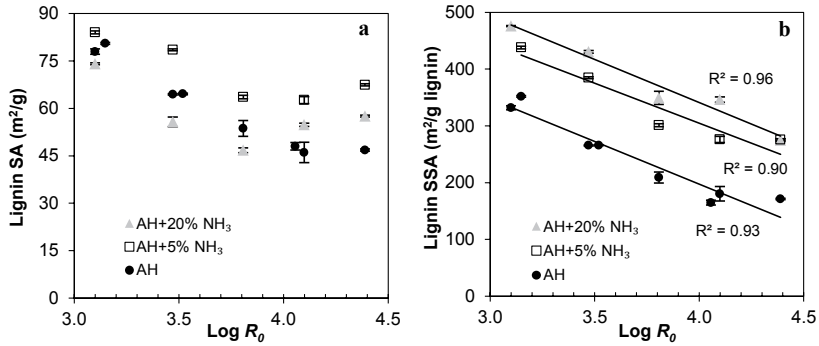

Figure 30. Effect of wheat straw autohydrolysis (AH) severity (Log R_0) on: **(a)** lignin surface area (SA); **(b)** lignin specific surface area (SSA). Solid residues from AH (circles) or from AH with subsequent extraction with 5% NH_3 (aq) at 140 °C (squares) or 20% NH_3 (aq) at 160 °C (triangles) were characterized. Errorbars represent average deviations from the mean values calculated from duplicate experiments (**V**).

The mechanism of lignin coalescence during thermochemical pretreatment of maize stalk has been previously proposed (Donohoe *et al.*, 2008). In the current thesis, the tentative mechanism is extended to include the simultaneous changes found to occur in wheat straw LCN as a function of AH severity. The proposed mechanism of lignin densification is schematically shown in Fig. 31. Acid-catalyzed hydrolysis of hemicellulose liberates lignin fragments from the LCN surrounding cellulose microfibrils. This is the key initial step in the sequence leading to aggregation of lignin, because associated lignin molecules form homogeneous material which coalesces and migrates onto particle surfaces through an extrusion-type process when temperature is increased above glass transition temperature (T_g) of lignin. Cleavage of lignin aryl ether linkages, generation of new lignin C−C bonds, and accumulation of carbohydrate degradation products occur more readily as the severity increases. Resinous degradation products can be incorporated to lignin either via covalent linkages or as a result of co-precipitation with soluble lignin fragments when temperature is decreased. These changes lead to generation of spheres on the surfaces, distinguishable in the electron micrographs (Fig. 2 in **V**). The consequence of the above process is drastically modified chemical and especially morphological structure of lignin. The generated dense lignin aggregates form hydrophobic barrier to the dye Azure B in wheat straw solid residues. Consequential effects on cellulose accessibility seem likely as well. It has been previously speculated that lignin droplets deposited during dilute acid pretreatment retard enzymatic hydrolysis of cellulose (Selig *et al.*, 2007). On the other hand, localisation of lignin to a more concentrated distribution was later proposed to increase accessibility of cellulose microfibrils (Donohoe *et*

al., 2008). In order to elucidate between these conflicting views, the effect of lignin structure on enzymatic hydrolysis following the pretreatment was determined.

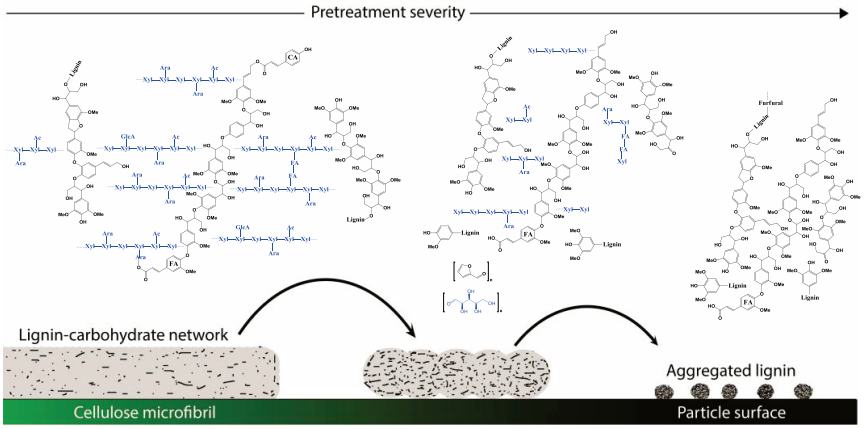

Figure 31. Proposed mechanism of lignin densification as a result of acid-catalyzed pretreatment. Lignin-carbohydrate network is hydrolytically depolymerized, leading to association and melting of lignin. Cleavage of aryl ether linkages releases soluble lignin fragments which react further with lignin or with furfural forming aggregates on the particle surfaces (unpublished work).

4.6 Effect of altered lignin structure on enzymatic hydrolysis of wheat straw cellulose[(V)]

Enzymatic digestibility of cellulose after wheat straw autohydrolysis (AH) and extraction was previously correlated with lignin content or lignin surface area (Fig. 4 in **V**). Solid residues from AH only or AH with subsequent NH_3 (aq) extraction (two-stage process) were comparatively investigated. Here, a more detailed linear regression analysis was undertaken in order to reveal the impact of various structural features of the solid residues on enzymatic cellulose conversion (Fig. 32). After AH, inverse correlation with cellulose conversion was obtained with hemicellulose content (R^2=0.99), lignin surface area (R^2=0.92) or lignin structure (R^2=0.81), whereas positive correlation was obtained with cellulose content (R^2=0.89) and unexpectedly also with increasing lignin content (R^2=0.68). After the two-stage process, lower levels of correlations were obtained in general. Interestingly, hemicellulose content no longer correlated with cellulose digestibility, and the correlation with lignin content was reversed from positive to negative (R^2=0.42). In contrast, consistent negative correlation after either of the two processes was obtained with lignin SA which also gave the highest correlation with cellulose conversion after the two-stage process (R^2=0.46). Therefore, processing in the contrastive conditions elaborately revealed that lignin SA was the most reliable explanatory factor among those evaluated. The importance of this observation

is obvious since previously lignin content has been regarded as the main negative factor limiting enzymatic digestibility of cellulose. Moreover, this is the first time chemical and physical structure of lignin were systematically put into relation with hydrothermal pretreatment severity and subsequent cellulose hydrolysis.

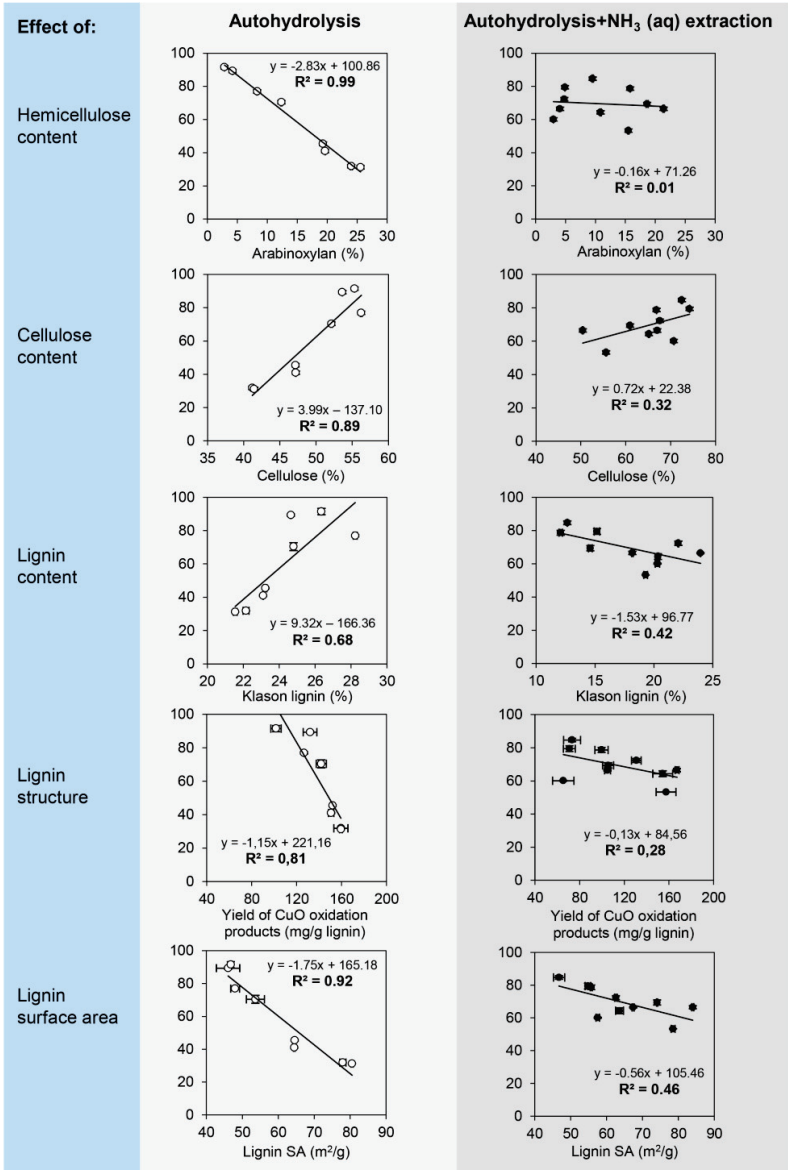

Figure 32. Enzymatic cellulose conversion (%, vertical axes) in 24 h hydrolysis (15 FPU/g) as a function of various properties of the solid residues before enzymatic hydrolysis. Correlation of solid residues from autohydrolysis (AH) only or AH with additional NH_3 (aq) extraction is shown. The errorbars represent average deviation from the mean values obtained from duplicate experiments (**V** and unpublished work).

5 Discussion

5.1 Relevance of the results regarding development of improved lignocellulose pretreatment processes for biorefineries

The current thesis investigated the effect of chemical, mechanical, hydrothermal, and thermochemical treatments of maize stem and wheat straw on lignin structure. The revealed impacts of acid- and base-catalyzed pretreatments on grass lignin were contrastive. The former caused cleavage and densification of lignin in the insoluble fraction, whereas the latter led to partial disaggregation and dissolution of lignin. Alkaline extraction alone dissolved two thirds of maize stem lignin at room temperature, whereas depolymerization of lignin occurred at 160 ºC. Pretreatment may induce many other changes in the lignocellulosic material such as increased porosity due to the solubilization of hemicelluloses and lignin. In fact, hemicellulose removal has been repeatedly correlated to cellulose conversion (Moxley *et al.*, 2012) and even suggested to be more important than removal of lignin for improving digestibility of cellulose (Mussatto *et al.*, 2008; Leu and Zhu, 2013). Enzymatic hydrolysis of cellulose has been recommended to be carried out using mixtures of cellulases supplemented with hemicellulases (Öhgren *et al.*, 2007). However, while the enzymatic hydrolysis reactions of the present work were carried out in the presence of xylanase activity, hemicellulose content did not correlate with cellulose digestibility after alkaline extraction of autohydrolysis solid residues. Moreover, according to the previously unpublished results, a linear correlation (R^2=0.89) was found between enzymatic conversions of arabinoxylan and cellulose among the 19 wheat straw solid fractions analyzed. Therefore, accessibility of hemicellulose and cellulose evolved in parallel during the pretreatments. The underlying effect of hemicellulose removal in enzymatic hydrolysis might thus be explained by the cleavage of lignin-carbohydrate linkages and associated changes in lignin which increased accessibility of cellulose in the solid fraction. Reduction of lignin surface area occurs as a consequence of depolymerization of the lignin-carbohydrate network. The area occupied by lignin is the most important change in lignin because it governs the proportion of accessible cellulose. Summing up, an optimum pretreatment would cleave lignin-carbohydrate linkages and decrease the area occupied by lignin. These phenomena explain why autohydrolysis and other hydrothermal processes are effective pretreatments even though they do not cause notable delignification. In spite of the effort placed in avoiding hemicellulose degradation through development of two-stage pretreatments comprising autohydrolysis and subsequent

delignification (Lora and Wayman, 1978; Huijgen *et al.*, 2012; **IV**−**V**), it might be worthwhile to conduct the two steps in the inverse order on grass feedstock. First, a majority of lignin and lignin-carbohydrate linkages would be cleaved by alkaline extraction, and in the second step the residual lignin in the solid fraction would be subjected to a short high temperature treatment in order to reduce surface area of the residual lignin.

5.2 Assessment of surface areas of lignocellulose

Accessible surface area (SA) of lignin was determined in three crop residues using the dye adsorption method (**III**). The obtained lignin surface areas (48–84 m^2/g, Table 5) were higher than total surface areas of lignocellulosic materials reported in the literature using different techniques. For instance, Brunauer–Emmett–Teller (BET) nitrogen physisorption analysis has given 0.64 m^2/g total SA for wheat straw, which was only increased to 2.3 m^2/g after ball milling (Gharpuray *et al.*, 1983). Higher SA for wheat straw was obtained by the nitrogen adsorption (3.3 m^2/g) and substantially higher SA by mercury intrusion porosimetry (38 m^2/g) (Chesson *et al.*, 1997). Spruce wood fractions at differing particle sizes showed almost similar SA (19–29 m^2/g) when determined using methylene blue and nitrogen adsorption, but the former gave multiple times higher SA (78–122 m^2/g) for peat that contains acidic groups arising from lignin (Poots and McKay, 1979). In fact, the nitrogen adsorption method has been suggested to underestimate SA of peat (Sun and Yang, 2003) or lignocellulosic materials by the factor of 10–15 (Chundawat *et al.*, 2011). This discrepancy might arise partially from the fact that the BET gas adsorption analysis requires the test material to be completely dry, which is often achieved by drying at 150 °C (Sun and Yang, 2003). However, drying at high temperature induces cell wall shrinkage, tissue deformation (Maziero *et al.*, 2013), and hornification which is the process of collapse and irreversible attachment of porous structures (Östlund *et al.*, 2010). This would adversely affect cellulase mobility in the material (Hendriks and Zeeman, 2009). Evidently, it would be important to determine the surface properties of lignocellulose in wet state. Thermoporometry has been used to measure pore volume distribution of lignocellulose (Ishizawa *et al.*, 2007). Although this technique could be used to determine the total pore surface area, qualitative surface composition has not been reported. Specific surface area of cellulose has been measured by adsorption of non-hydrolytic protein on pure cellulose materials (2.4–42 m^2/g), and Congo Red on spruce (16 m^2/g) (Hong *et al.*, 2007; Wiman *et al.*, 2012). Yet, there is little information of surface properties of plant residues in general and SA of lignin in particular. Among the few publications, calculative surface areas of lignin particles were reported between 0.5–60 m^2/g based on X-ray scattering (Vainio *et al.*, 2004). The quantitative dye adsorption method enables characterization of surface-accessible lignin in aqueous suspension at neutral pH, which is a key advantage of this technique.

In the best knowledge of the author, the results in **III** were the first reported values of lignin surface areas based on direct probing at the molecular level.

5.3 Heterogeneous distribution of lignin in grasses and its technical and analytical implications

The effect of physicochemical pretreatment or extraction of lignocellulose on lignin structure is often evaluated relative to either lignin in the untreated material or reference lignin isolated using literature procedures (Björkman, 1956; Lundqvist, 1992b; Wu and Argyropoulos, 2003). These comparisons are valid only if distribution of lignin across the material is homogeneous (Fig. 33). However, the structure of grass lignin depends on the depth of extraction as demonstrated by the fractions isolated sequentially from maize stem by dilute alkali at room temperature (**I**). The first mild alkaline extraction dissolved lignin mainly from the ML and CC regions, the recovered fraction accounting for 39% of the initial lignin. The second fraction accounted for 8% of the initial lignin, but since it was obtained after treatment with endoglucanase, it was likely originating from the P and S regions of the cell walls. The distinctly high proportion of β-O-4 bonds and **S** units in the first fraction suggest that lignin is heterogeneously distributed across the maize stem cell wall regions (Fig. 33). Consistently, alkaline extraction of wheat straw after autohydrolysis removed lignin enriched in **S** units (Fig. 28b). Similar trend can be expected for other grasses, but in order to confirm this further work is needed to systematically fractionate and characterise lignin. The sequential extraction procedure can be used to isolate fractions of interest for structure-relationship analyses.

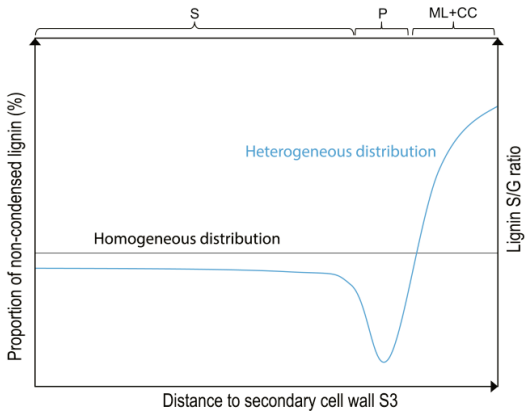

Figure 33. Scheme of possible linear and non-linear distribution of non-condensed lignin and relative proportions of **S** and **G** units of lignin (**S**/**G** ratio) across the grass cell wall regions (S, secondary cell wall; P, primary cell wall, ML, middle lamella, CC, cell corner) (unpublished work).

6 Conclusions and future prospects

The general objective of this work was to elucidate the effect of a variety of treatments on grass lignin structure and its subsequent effect on enzymatic hydrolysis of cellulose. The implemented experiments consisted of analysis of plant residues of industrial and agronomical interest after chemical, mechanical, and physicochemical treatments and consequential enzymatic digestibility of carbohydrates. This approach turned out to be rewarding because simultaneous changes in carbohydrates and lignin could be identified and used to make firm conclusions.

From the knowledge perspective one of the key results of the thesis was the unveiling of the tendency of lignin enriched in non-condensed syringyl units to dissolve when maize stem or wheat straw materials were extracted with aqueous alkali. Heterogeneity of lignin is not itself a new concept, but it is important that the developed sequential fractionation procedure enabled proposing a schematic distribution of lignin in the grass cell wall regions for the first time. Moreover, considerable proportion of lignin can be recovered in two fractions containing distinct lignin structures.

It is interesting that the first alkali-soluble fraction can account for more than two thirds of the total lignin of grasses. This mobility of lignin might be a universal strategy evolved in plants as a barrier against enzymatic hydrolysis of cellulose. The key component in this recalcitrance is the lignin-carbohydrate network (LCN). Its impeding effect on enzymatic digestibility of maize stem carbohydrates was concluded to be caused by lignin-carbohydrate linkages that resisted ball milling at high intensity as long as 12 h. These results disfavor milling as the sole pretreatment for grass lignocellulose.

From the methodological point of view, one of the most important advances brought by this work was the development of the quantitative method for determination of surface-accessible acidic hydroxyl groups and surface area of lignin in lignocellulosic materials. Consequently, structural changes in wheat straw lignin were determined as a function of autohydrolysis severity and as a result of alkaline extractions. Inverse linear correlation was found between lignin surface area and enzymatic hydrolysis of cellulose. This is the first time the detrimental effect of lignin on cellulose digestibility was experimentally evidenced to arise from the morphological structure of lignin.

From the technological perspective, this work underscores that it is important to take into account structural changes in lignin during various pretreatments. Hydrolysis of the grass LCN in acidic conditions liberates lignin fragments which associate, depolymerize and aggregate on solid residues. The resulting lignin resists alkaline extraction and adopts denser solid-state structure compared to lignin isolated without acidic pretreatment. Enzymatic hydrolysis of lignocellulosic substrates would deserve further investigations in order to

determine the kinetic changes on lignocellulosic surfaces. With respect to the surface properties, opportunities exist in the use of spectroscopic techniques in parallel with the wet-chemistry tools for assessing enzymatic digestibility of cellulose and for improving efficacy of the existing and novel pretreatment processes. In addition to probing accessible cellulose, the determination of lignin surface area should turn out valuable in these undertakings.

7 References

Adler, E. Lignin chemistry - past, present and future. *Wood Sci. Technol.* **11** (1977) 169–218.

Allen, S.J., McKay, G., Khader, K.Y.H. Intraparticle diffusion of a basic dye during adsorption onto sphagnum peat. *Environ. Pollut.* **56** (1989) 39–50.

Alvira, P., Tomás-Pejó, E., Ballesteros, M., Negro, M.J. Pretreatment technologies for an efficient bioethanol production process based on enzymatic hydrolysis: A review. *Bioresour. Technol.* **101** (2010) 4851–4861.

Anon, http://www.nasdaq.com/markets/ethanol.aspx, accessed 19.2.2015.

Argyropoulos, D.S. Personal communication, 05.11.2014.

Atalla, R.H.; VanderHart, D.L. Native Cellulose: A Composite of Two Distinct Crystalline Forms. *Science* **223** (1984) 283–285.

Balakshin, M., Capanema, E., Gracz, H., Chang, H.-M., Jameel, H. Quantification of lignin–carbohydrate linkages with high-resolution NMR spectroscopy. *Planta* **233** (2011) 1097–1110.

Barakat, A., de Vries, H., Rouau, X. Dry fractionation process as an important step in current and future lignocellulose biorefineries: A review. *Biores. Tehcnol.* **134** (2013) 362–373.

Baumberger, S., Abaecherli, A., Fasching, M., Gellerstedt, G., Gosselink, R., Hortling, B., Li, J., Saake, B., de Jong, E. Molar mass determination of lignins by size-exclusion chromatography: towards standardisation of the method. *Holzforschung* **61** (2007) 459–468.

Bayer, E.A., Kenig, R., Lamed, R. Adherence of Clostridium thermocellum to Cellulose. *J. Bacteriol.* **156** (1983) 818–827.

Behera, S., Arora, R., Nandhagopal, N., Kumar, S. Importance of chemical pretreatment for bioconversion of lignocellulosic biomass. *Renew. Sust. Energ. Rev.* **36** (2014) 91–106.

Bidlack, J., Malone, M., Benson, R. Molecular structure and component integration of secondary cell walls in plants. *Proc. Okla. Acad. Sci.* **72** (1992) 51–56.

Binder, J.B., Raines, R.T. Fermentable sugars by chemical hydrolysis of biomass. *PNAS* **107** (2010) 4516–4521.

Björkman, A. Finely divided wood. I. Extraction of lignin with neutral solvents. *Svensk Papperstidn.* **59** (1956) 477–485.

Björkman, A. Lignin and Lignin-Carbohydrate Complexes. *Ind. Eng. Chem.* **49** (1957) 1395–1398.

Bocchini, P., Galletti, G.C., Camarero, S., Martinez, A.T. Absolute quantitation of lignin pyrolysis products using an internal standard. *J. Chromatog. A* **773** (1997) 227–232.

Boerjan, W., Ralph, J., Baucher, M. Lignin Biosynthesis. *Annu. Rev. Plant. Biol.* **S4** (2003) 519–546.

Boon, E.J.M.C., Struik, P.C., Engels, F.M., Cone, J.W. Stem characteristics of two forage maize (*Zea mays* L.) cultivars varying in whole plant digestibility. IV. Changes during the growing season in anatomy and chemical composition in relation to fermentation characteristics of a lower internode. *Neth. J. Agric. Sci.* **59** (2012) 13–23.

Boraston, A.B., Bolam, D.N., Gilbert, H.J., Davies, G.J. Carbohydrate-binding modules: fine-tuning polysaccharide recognition. *Biochem. J.* **382** (2004) 769–781.

Bradford, M.M. A rapid and sensitive method for quantitation of microgram quantities of protein utilizing the principle of protein-dye-binding. *Anal. Biochem.* **72** (1976) 248–254.

Bu, L., Beckham, G.T., Crowley, M.F., Chang, C.H., Matthews, J.F., Bomble, Y.J., Adney, W.S., Himmel, M.E., Nimlos, M.R. *J. Phys. Chem. B* **113** (2009) 10994–11002.

Cathala, B., Saake, B., Faix, O., Monties, B. Association behaviour of lignins and lignin model compounds studied by multidetector size-exclusion chromatography. *J. Chromatogr. A* **1020** (2003) 229–239.

Carvalheiro, F., Silva-Fernandes, T., Duarte, L.C., Gírio, F.M. Wheat Straw Autohydrolysis: Process Optimization and Products Characterization. *Appl. Biochem. Biotechnol.* **153** (2009) 84–93.

Chen, C.-L., Nitrobenzene and cupric oxide oxidations. In: *Methods in Lignin Chemistry*, C.W. Dence, S.Y. Lin (eds.), Springer-Verlag, Berlin, 1992, pp. 301–321.

Chen, F., Dixon, R.A. Lignin modification improves fermentable sugar yields for biofuel production. *Nature Biotechnol.* **25** (2007) 759–761.

Chen, F.C., Li, J., Aqueous gel permeation chromatographic methods for technical lignins. *J. Wood Chem. Technol.* **20** (2000) 265–276.

Chesson, A., Gardner, P.T., Wood, T.J. Cell wall porosity and available surface area of wheat straw and wheat grain fractions. *J. Sci. Food Agric.* **75** (1997) 289–295.

Chundawat, S.P.S., Donohoe, B.S., Sousa, L.D., Elder, T., Agarwal, U.P., Lu, F., Ralph, J., Himmel, M.E., Balan, V., Dale, B.E. Multi-scale visualization and characterization of lignocellulosic plant cell wall deconstruction during thermochemical pretreatment. *Energy Environ. Sci.* **4** (2011) 973–984.

Coletta, V.C., Rezende, C.A., da Conceição, F.R., Polikarpov, I., Guimarães, F.E.G. Mapping the lignin distribution in pretreated sugarcane bagasse by confocal and fluorescence lifetime imaging microscopy. *Biotechnol. Biofuels* (2013) **6**:43.

Connolly, M.L. Analytical molecular surface calculation. *J. Appl. Cryst.* **16** (1983) 548–558.

Converse, A.O., Matsuno, R., Tanaka, M., Taniguchi, M. A model of enzyme adsorption and hydrolysis of microcrystalline cellulose with slow deactivation of the adsorbed enzyme. *Biotechnol. Bioeng.* **32** (1988) 38–45.

Cornu, A., Besle, J.M., Mosoni, P., Grenet, E. Lignin-carbohydrate complexes in forages: structure and consequences in the ruminal degradation of cell-wall carbohydrates. *Reprod. Nutr. Dev.* **34** (1994) 385–398.

Côté, W.A. *Wood Ultrastructure*., University of Washington Press, New York, NY, USA, 1967.

Crestini, C., Argyropoulos, D.S. Structural analysis of wheat straw lignin by quantitative ^{31}P and 2D NMR spectroscopy. The occurrence of ester bonds and α-O-4 substructures. *J. Agric. Food Chem.* **45** (1997) 1212–1219.

Crestini, C., Melone, F., Sette, M., Saladino, R. Milled wood lignin: a linear oligomer. *Biomacromolecules* **12** (2011) 3928–3935.

Culhaoglu, T., Zheng, D., Méchin, V., Baumberger, S. Adaptation of the Carrez procedure for the purification of ferulic and *p*-coumaric acids released from lignocellulosic biomass prior to LC/MS analysis. *J. Chromatogr., B* **879** (2011) 3017–3022.

Dale, B.E., Leong, C.K., Pham, T.K., Esquivel, V.M., Rios, I., Latimer, V.M. Hydrolysis of lignocellulosics at low enzyme levels: application of the AFEX process. *Bioresour. Technol.* **56** (1996) 111–116.

Danon, B., van der Aa, L., de Jong, W. Furfural degradation in a dilute acidic and saline solution in the presence of glucose. *Carbohydr. Res.* **375** (2013) 145–152.

del Río, J.C., Rencoret, J., Prinsen, P., Martinez, A.T., Ralph, J., Gutierrez, A. Structural characterization of wheat straw lignin as revealed by analytical pyrolysis, 2D-NMR, and reductive cleavage methods. *J. Agric. Food Chem.* **60** (2012) 5922–5935.

Dence, C.W., The determination of lignin. In: *Methods in Lignin Chemistry*, C.W. Dence, S.Y. Lin (eds.), Springer-Verlag, Berlin, Germany, 1992, pp. 33–61.

Dervilly, G., Saulnier, L., Roger, P., Thibault, J.-F. Isolation of homogeneous fractions from wheat water-soluble arabinoxylans. Influence of the structure on their macromolecular characteristics. *J. Agric. Food Chem.* **48** (2000) 270–278.

Dimmel, D.R., Overview. In: *Lignin and Lignans: Advances in Chemistry*, C. Heitner, D.R. Dimmel, J.A. Schmidt (eds.), CRC Press, Boca Raton, FL, USA, 2010, pp. 1–10.

Donaldson, L., Hague, J., Snell, R. Lignin distribution in coppice poplar, linseed and wheat straw. *Holzforschung* **55** (2001) 379–385.

Donohoe, B.S., Decker, S.R., Tucker, M.P., Himmel, M.E., Vinzant, T.B. Visualizing lignin coalescence and migration through maize cell walls following thermochemical pretreatment. *Biotechnol. Bioeng.* **101** (2008) 913–925.

Ebringerová, A., Hromádková, Z., Alföldi, J., Berth, G. Structural and solution properties of corn cob heteroxylans. *Carbohydr. Polym.* **19** (1992) 99–105.

Ebringerová, A., Hromádková, Z., Heinze, T. Hemicellulose. *Adv. Polym. Sci.* **186** (2005) 1–67.

Esteghlalian, A., Hashimoto, A.G., Fenske, J.J., Penner, M.H. Modeling and optimization of the dilute-sulfuric-acid pretreatment of corn stover, poplar and switchgrass. *Bioresour. Technol.* **59** (1997) 129–136.

Esterbauer, H., Steiner, W., Labudova, I., Hermann, A., Hayn, M. Production of *Trichoderma* cellulase in laboratory and pilot scale. *Bioresour. Technol.* **36** (1991) 51–65.

Fan L.T., Gharpuray M.M., Lee Y.H. Biotechnology Monographs – Cellulose Hydrolysis, vol. 3. Springer, New York, NY, USA, 1987, 198 p.

Fan, L.T., Lee, Y-H., Gharpuray, M.M. The nature of lignocellulosics and their pretreatments for enzymatic hydrolysis. *Adv. Biochem. Eng.* **23** (1982) 157–87.

Fidalgo, M.L., Terrón, M.C., Martínez, A.T., González, A.E., González-Vila, F.J., Galletti, G.C. Comparative study of fractions from alkaline extraction of wheat straw through chemical degradation, analytical pyrolysis, and spectroscopic techniques. *J. Agric. Food Chem.* **41** (1993) 1621–1626.

Forsberg, Z., Vaaje-Kolstad, G., Westereng, B., Bunæs, A.C., Stenstrøm, Y., MacKenzie, A., Sørlie, M., Horn, S.J., Eijsink, V.G.H. Cleavage of cellulose by a CBM33 protein. *Protein Sci.* **20** (2011) 1479–1483.

Freudenberg, K. and Neish, A.C. *Constitution and Biosynthesis of Lignin*. Springer-Verlag, Berlin, Germany, 1968, 129 p.

Galbe, M., Zacchi, G. Pretreatment: The key to efficient utilization of lignocellulosic materials. *Biomass Bioenergy* **46** (2012) 41–65.

Gao, D., Chundawat, S.P.S., Sethi, A., Balan, V., Gnanakaran, S., Dale, B.E. Increased enzyme binding to substrate is not necessary for more efficient cellulose hydrolysis. *PNAS* **110** (2013) 10922–10927.

Garrote, G., Dominguez, H., Parajó, J.C. Hydrothermal processing of lignocellulosic materials. *Holz Roh- Werkst.* **57** (1999) 191–202.
Garrote, G., Dominguez, H., Parajó, J.C. Kinetic modelling of corncob autohydrolysis. *Process Biochem.* **36** (2001) 571–578.
Geddes, C.C., Nieves, I.U., Ingram, L.O. Advances in ethanol production. *Curr. Opin. Biotechnol.* **22** (2011) 312–319.
Gharpuray, M.M., Lee, Y.-H., Fan, L.T. Structural modification of lignocellulosics by pretreatments to enhance enzymatic hydrolysis. *Biotechnol. Bioeng.* **25** (1983) 157–172.
Ghose, T.K., Measurement of cellulase activities. *Pure Appl. Chem.* **59** (1987) 257–268.
Gosselink, R.J.A., Abächerli, A., Semke, H., Malherbe, R., Käuper, P., Nadif, A., van Dam, J.E.G. Analytical protocols for characterization of sulphur-free lignin. *Ind. Crops Prod.* **19** (2004) 271–281.
Grabber, J.H., Hatfield, R.D., Ralph, J., Zón, J., Amrhein, N., Ferulate cross-linking in cell walls isolated from maize cell suspensions. *Phytochem.* **40** (1995) 1077–1082.
Grabber, J.H., Ralph, J., Hatfield, R.D., Quideau, S. p-Hydroxyphenyl, Guaiacyl, and Syringyl Lignins Have Similar Inhibitory Effects on Wall Degradability. *J. Agric. Food Chem.* **45** (1997) 2530–2532.
Grabber, J.H., Ralph, J., Lapierre, C., Barrière, Y. Genetic and molecular basis of grass cell-wall degradability. I. Lignin–cell wall matrix interactions. *C. R. Biologies* **327** (2004) 455–465.
Granata, A., Argyropoulos, D.S. 2-Chloro-4,4,5,5-tetramethyl-1,3,2-dioxaphospholane, a reagent for the accurate determination of the non-condensed and condensed phenolic moieties in lignins. *J. Agric. Food Chem.* **43** (1995) 1538–1544.
Guerra, A., Filpponen, I., Lucia, L.A., Saquing, C., Baumberger, S., Argyropoulos, D.S. Toward a better understanding of the lignin isolation process from wood. *J. Agric. Food Chem.* **54** (2006) 5939–5947.
Hale, J.D. Structural and physical properties of pulpwood. In: *Pulp and paper manufacture, The pulping of wood*, R.G. MacDonald and J.N. Franklin (eds.) 2nd edition vol. 1, McGraw-Hill, New York, NY, USA, 1969, p. 14.
Hansen, M.A.T., Hidayat, B.J., Mogensen, K.K., Jeppesen, M.D., Jørgensen, B., Johansen, K.S., Thygesen, L.G., Enzyme affinity to cell types in wheat straw (*Triticum aestivum* L.) before and after hydrothermal pretreatment. *Biotechnol. Biofuels* (2013) **6**:54.
Harris, P.J., Hartley, R.D. Detection of bound ferulic acid in cell walls of the Gramineae by ultraviolet fluorescence microscopy. *Nature* **259** (1976) 508–510.
Heikkinen, H., Elder, T., Maaheimo, H., Rovio, S., Rahikainen, J., Kruus, K., Tamminen, T. Impact of steam explosion on the wheat straw lignin structure studied by solution-state nuclear magnetic resonance and density functional methods. *J. Agric. Food Chem.* **62** (2014) 10437–10444.
Heiss-Blanquet, S., Zheng, D., Ferreira, N.L., Lapierre, C., Baumberger, S. Effect of pretreatment and enzymatic hydrolysis of wheat straw on cell wall composition, hydrophobicity and cellulase adsorption. *Bioresour. Technol.* **102** (2011) 5938–5946.
Hendriks, A.T.W.M., Zeeman, G. Pretreatments to enhance the digestibility of lignocellulosic biomass. *Bioresour. Technol.* **100** (2009) 10–18.

Hideno, A., Inoue, H., Tsukahara, K., Fujimoto, S., Minowa, T., Inoue, S., Endo, T., Sawayama, S. Wet disk milling pretreatment without sulfuric acid for enzymatic hydrolysis of rice straw. *Bioresour. Technol.* **100** (2009) 2706–2711.

Higuchi, T., Tanahashi, M., Nakatsubo, F. Acidolysis of bamboo lignin. III. Estimation of arylglycerol-β-aryl ether groups in lignins. *Wood Res.* **54** (1972) 9–18.

Himmel, M.E., Ding, S.-Y., Jonhson, D.K., Adney, W.S., Nimlos, M.R., Brady, J.W., Foust, T.D. Biomass Recalcitrance: Engineering Plants and Enzymes for Biofuels Production. *Science* **315** (2007) 804–807.

Hoeger, I.C., Filpponen, I., Martin-Sampedro, R., Johansson, L.-S., Österberg, M., Laine, J., Kelley, S., Rojas, O.J. Bicomponent Lignocellulose Thin Films to Study the Role of Surface Lignin in Cellulolytic Reactions. *Biomacromolecules* **13** (2012) 3228–3240.

Holopainen-Mantila, U., Marjamaa, K., Merali, Z., Käsper, A., de Bot, P., Jääskeläinen, A.-S., Waldron, K., Kruus, K., Tamminen, T. Impact of hydrothermal pre-treatment to chemical composition, enzymatic digestibility and spatial distribution of cell wall polymers. *Bioresour. Technol.* **138** (2013) 156–162.

Hong, J., Ye, X., Zhang, Y.-H.P. Quantitative Determination of Cellulose Accessibility to Cellulase Based on Adsorption of a Nonhydrolytic Fusion Protein Containing CBM and GFP with Its Applications. *Langmuir* **23** (2007) 12535–12540.

Huijgen, W.J.J., Smit, A.T., de Wild, P.J., den Uil, H. Fractionation of wheat straw by prehydrolysis, organosolv delignification and enzymatic hydrolysis for production of sugars and lignin. *Bioresour. Technol.* **114** (2012) 389–398.

Igarashi, K., Uchihashi, T., Koivula, A., Wada, M., Kimura, S., Okamoto, T., Penttilä, M., Ando, T., Samejima, M. Traffic jams reduce hydrolytic efficiency of cellulase on cellulose surface. *Science* **333** (2011) 1279–1282.

Iiyama, K., Lam, T.B.-T., Stone, B.A. Covalent cross-links in the cell wall. *Plant Physiol.* **104** (1994) 315–320.

Ishii, T. Isolation and characterization of a diferuloyl arabinoxylan hexasaccharide from bamboo shoot cell walls. *Carbohydr. Res.* **219** (1991) 15–22.

Ishizawa, C.I., Davis, M.F., Schell, D.F., Johnson, D.K. Porosity and its effect on the digestibility of sulfuric acid pretreated corn stover. *J. Agric. Food Chem.* **55** (2007) 2575–2581.

Jacquet, G., Pollet, B., Lapierre, C. New ether-linked ferulic acid-coniferyl alcohol dimers identified in grass straws. *J. Agric. Food Chem.* **43** (1995) 2746–2751.

Jeffries, T.W. Biodegradation of lignin-carbohydrate complexes. *Biodegradation* **1** (1990) 163–176.

Jung, H.G., Mertens, D.R., Payne, A.J. Correlation of acid detergent lignin and Klason lignin with digestibility of forage dry matter and neutral detergent fiber *J. Dairy Sci.* **80** (1997) 1622–1628.

Kim, E.S., Lee, H.J., Bang, W.-G., Choi, I.-G., Kim, K.H. Functional characterization of a bacterial expansin from *Bacillus subtilis* for enhanced enzymatic hydrolysis of cellulose. *Biotechnol. Bioeng.* **102** (2009) 1342–1353.

Kim, T.H., Lee, Y.Y. Fractionation of corn stover by hot-water and aqueous ammonia treatment. *Bioresour. Technol.* **97** (2006) 224–232.

Kondo, R., Tsutsumi, Y., Imamura, H. Kinetics of β-aryl ether cleavage of phenolic syringyl type lignin model compounds in soda and Kraft systems. *Holzforschung* **41** (1987) 83–88.

Koshijima, T., Watanabe, T. Association between lignin and carbohydrates in wood and other plant tissues. In: *Springer Series in Wood Science*; T.E. Timell (ed.), Springer-Verlag, Berlin, Germany, 2003, p. 329.

Kristensen, J.B., Thygesen, L.G., Felby, C., Jørgensen, H., Elder, T. Cell-wall structural changes in wheat straw pretreated for bioethanol production. *Biotechnol. Biofuels* (2008) **1**:5.

Langmuir, I. The constitution and fundamental properties of solids and liquids. Part I. Solids. *J. Am. Chem. Soc.* **38** (1916) 2221–2295.

Lapierre, C., Jouin, D. and Monties, B., On the molecular origin of the alkali solubility of gramineae lignins. *Phytochem.* **28** (1989) 1401–1403.

Lawoko, M. Lignin Polysaccharide Networks in Softwood and Chemical Pulps: Characterization, Structure and Reactivity. Doctoral thesis, KTH, Stockholm, Sweden, 2005, 58 p.

Lawther, J.M., Sun, R.-C. Banks, W.B., Rapid Isolation and structural characterization of alkali-soluble lignins during alkaline treatment and atmospheric refining of wheat straw, *Ind. crop Prod.* **5** (1996) 97–105.

Laurichesse, S., Avérous, L. Chemical modification of lignins: Towards biobased polymers. *Prog. Polym. Sci.* **39** (2014) 1266–1290.

Le Costaouëc, T., Pakarinen, A., Várnai, A., Puranen, T., Viikari, L. The role of carbohydrate binding module (CBM) at high substrate consistency: Comparison of Trichoderma reesei and Thermoascus aurantiacus Cel7A (CBHI) and Cel5A (EGII). *Bioresour. Technol.* **143** (2013) 196–203.

Leu, S.-Y., Zhu, J.Y. Substrate-related factors affecting enzymatic saccharification of lignocelluloses: our recent understanding. *Bioenerg. Res.* **6** (2013) 405–415.

Li, J., Henriksson, G., Gellerstedt, G. Lignin depolymerization/repolymerization and its critical role for delignification of aspen wood by steam explosion. *Bioresour. Technol.* **98** (2007) 3061–3068.

Li, H., Pu, Y., Kumar, R., Ragauskas, A.J., Wyman, C.E. Investigation of lignin deposition on cellulose during hydrothermal pretreatment, its effect on cellulose hydrolysis, and underlying mechanisms. *Biotechol. Bioeng.* **111** (2014) 485–492.

Liu, R., Yu, H., Huang, Y. Structure and morphology of cellulose in wheat straw. *Cellulose* **12** (2005) 25–34.

Lora, J. Industrial Commercial Lignins: Sources, Properties and Applications. In: *Monomers, Polymers and Composites from Renewable Resources*, M.N. Belgacem, A. Gandini, (Eds.), Elsevier, Amsterdam, The Netherlands, 2008, pp. 225-241.

Lora, J., Wayman, M., Delignification of hardwoods by autohydrolysis and extraction. *Tappi J.* **61** (1978) 47–50.

Lu, F., Ralph, J. Non-degradative dissolution and acetylation of ball-milled plant cell walls: high resolution solution-state NMR. *Plant J.* **35** (2003) 535–544.

Lundqvist, K. Acidolysis. In: *Methods in Lignin Chemistry*, C.W. Dence, S.Y. Lin (eds.), Springer-Verlag, Berlin, Germany, 1992a, pp. 289–300.

Lundquist, K. Isolation and purification: Wood. In: *Methods in Lignin Chemistry*, C.W. Dence, S.Y. Lin (eds.), Springer-Verlag, Berlin, 1992b, Germany, pp. 65–70.

Lynd, L.R., Laser, M.S., Bransby, D., Dale, B.E., Davidson, B., Hamilton, R., Himmel, M., Keller, M., McMillan, J.D., Sheehan, J., Wyman, C.E. How biotech can transform biofuels. *Nat. Biotechnol.* **26** (2008) 169–172.

Lynd, L.R., Weimer, P.J., van Zyl, W.H., Pretorius, I.S. Microbial cellulose utilization: fundamentals and biotechnology. *Microbiol. molecul. biol. rev.* **66** (2002) 506-577.

Mansfield, S.D., Mooney, C., Saddler, J.N. Substrate and enzyme characteristics that limit cellulose hydrolysis. *Biotechnol. Prog.* **15** (1999) 804−816.

Martín-Sampedro, R., Rahikainen, J.L., Johansson, L.-S., Marjamaa, K., Laine, J., Kruus, K., Rojas, O.J. Preferential adsorption and activity of monocomponent cellulases on lignocellulose thin films with varying lignin content. *Biomacromolecules* **14** (2013) 1231−1239.

Maziero, P., Jong, J., Mendes, F.M., Goncalves, A.R., Eder, M., Driemeier, C. Tissue-specific cell wall hydration in sugarcane stalks. *J. Agric. Food Chem.* **61** (2013) 5841−5847.

McIntosh, S., Vancov, T. Optimisation of dilute alkaline pretreatment for enzymatic saccharification of wheat straw. *Biomass Bioenergy* **35** (2011) 3094–3103.

Méchin, V., Laluc, A., Legée, F., Cézard, L., Denoue, D., Barrière, Y., Lapierre, C. Impact of the Brown-Midrib bm5 mutation on maize lignins. *J. Agric. Food Chem.* **62** (2014) 5102−5107.

Mesa, L., González, E., Cara, C., González, M., Castro, E., Mussatto, S.I. The effect of organosolv pretreatment variables on enzymatic hydrolysis of sugarcane bagasse. *Chem. Eng. J.* **168** (2011) 1157–1162.

Miller, G.L. Use of dinitrosalicylic acid reagent for determination of reducing sugar. *Anal. Chem.* 31 (1959) 426–428.

Mood, S.H., Golfeshan, A.H., Tabatabaei, M., Jouzani, G.S., Najafi, G.H., Gholami, Ardjmand, M. Lignocellulosic biomass to bioethanol, a comprehensive review with a focus on pretreatment. *Renew. Sust. Energ. Rev.* **27** (2013) 77–93.

Montané, D., Farriol, X., Salvadó, J., Jollez, P., Chornet, E. Fractionation of wheat straw by steam-explosion pretreatment and alkali delignification. Cellulose pulp and byproducts from hemicellulose and lignin. *J. Wood Chem. Technol.* **18** (1998) 171–191.

Monteil-Rivera, F., Phuong, M., Ye, M., Halasz, A., Hawari, J., Isolation and characterization of herbaceous lignins for applications in biomaterials. *Ind. Crops Prod.* **41** (2013) 356–364.

Moxley, G., Gaspar, A.R., Higgins, D., Xu, H. Structural changes of corn stover lignin during acid pretreatment. *J. Ind. Micorbiol. Biotechnol.* **39** (2012) 1289–1299.

Mussatto, S.I., Fernandes, M., Milagres, A.M.F., Roberto, I.C. Effect of hemicellulose and lignin on enzymatic hydrolysis of cellulose from brewer's spent grain. *Enzyme Microb. Technol.* **43** (2008) 124–129.

Nabarlatz, D., Farriol, X., Montané, D. Kinetic modeling of the autohydrolysis of lignocellulosic biomass for the production of hemicellulose-derived oligosaccharides. *Ind. Eng. Chem. Res.* **43** (2004) 4124–4131.

Nakamura, S., Wakabayashi, K., Nakai, R., Aono, R., Horikoshi, K. Purification and some properties of an alkaline xylanase from alkaliphilic Bacillus sp. strain 41M-1. *Appl. Environ. Microbiol.* **59** (1993) 2311–2316.

Norgren, M., Edlund, H. Lignin: Recent advances and emerging applications. *Curr. Opin. Colloid Interface Sci.* **19** (2014) 409–416.

O'Connor, R.T., DuPré, E.F., Mitcham, D. Applications of infrared absorption spectroscopy to investigations of cotton and modified cottons. Part I: physical and crystalline modifications and oxidation. *Textile Res. J.* **28** (1958) 382–392.

O'Sullivan, A.C. Cellulose: the structure slowly unravels. *Cellulose* **4** (1997) 173–207.

Overend, R.P., Chornet, E. Fractionation of lignocellulosics by steam-aqueous pretreatments. *Philos. Trans. R. Soc*., **A321** (1987) 523–536.

Öhgren, K., Bura, R., Saddler, J., Zacchi, G. Effect of hemicellulose and lignin removal on enzymatic hydrolysis of steam pretreated corn stover. *Bioresour. Technol.* **98** (2007) 2503–2510.

Östlund, Å., Köhnke, T., Nordstierna, L., Nydén, M. NMR cryoporometry to study the fiber wall structure and the effect of drying. *Cellulose* **17** (2010) 321–328.

Paës, G., Burr, S., Saab, M.-B., Molinari, M., Aguié-Béghin, V., Chabbert, B., Modeling Progression of Fluorescent Probes in Bioinspired Lignocellulosic Assemblies. *Biomacromolecules* **14** (2013) 2196−2205.

Pakkanen, H., Alén, R. Molecular mass distribution of lignin from the alkaline pulping of hardwood , softwood, and wheat straw. *J. Wood Chem. Technol.* **32** (2012) 279–293.

Palmqvist, E., Hahn-Hägerdal, B. Fermentation of lignocellulosic hydrolysates. II: inhibitors and mechanisms of inhibition. *Bioresour. Technol.* **74** (2000) 25–33.

Pepper, J.M., Casselman, B.W., Karapally, J.C. Lignin oxidation. Preferential use of cupric oxide. *Can. J. Chem.* **45** (1967) 3009–3012.

Perlack, R.D., Eaton, L.M., Turhollow, A.F. Jr., Langholtz, M.H., Brandt, C.C., Downing, M.E., Graham, R.L., Wright, L.L., Kavkewitz, J.M., Shamey, A.M., Nelson, R.G., Stokes, B.J., Rooney, W.L., Muth, D.J. Jr., Hess, J.R, Abodeely, J.M., Hellwinckel, C., De La Torre Ugarte, D., Yoder, D.C., Lyon, J.P., Rials, T.G., Volk, T.A., Buchholz, T.S., Abrahamson, L.P., Anex, R.P., Voigt, T.B., Berguson, W., Riemenschneider, D.E., Karlen, D., Johnson, J.M.F., Mitchell, R.B., Vogel, K.P., Richard, E.P. Jr., Tatarko, J., Wagner, L.E., Skog, K.E., Lebow, P.K., Dykstra, D.P., Buford, M.A., Miles, P.D., Scott, D.A, Perdue, J.H., Rummer, R.B., Barbour, J., Stanturf, J.A., McKeever, D.B., Zalesny, R.S. Jr., Gee, E.A., Cassidy, P.D, Lightle, D., "U.S. Billion-ton Update: Biomass Supply for a Bioenergy and Bioproducts Industry", United States Department of Energy, 2011.

Pihlajaniemi, V., Sipponen, M.H., Pastinen, O., Lehtomäki, I., Laakso, S. Yield optimization and rational function modelling of enzymatic hydrolysis of wheat straw pretreated by NaOH-delignification, autohydrolysis and their combination. *Green Chem.* **17** (2015) 1683–1691.

Pihlajaniemi, V., Sipponen, S., Sipponen, M.H., Pastinen, O., Laakso, S. Enzymatic saccharification of pretreated wheat straw: Comparison of solids-recycling, sequential hydrolysis and batch hydrolysis. *Bioresour. Technol.* **153** (2014) 15–22.

Poots, V.J.P., McKay, G. The specific surfaces of peat and wood. *J. Appl. Polym. Sci.* **23** (1979) 1117–1129.

Rahikainen, J.L., Martin-Sampedro, R., Heikkinen, H., Rovio, S., Marjamaa, K., Tamminen, T., Rojas, O.J., Kruus, K. Inhibitory effect of lignin during cellulose bioconversion: The effect of lignin chemistry on non-productive enzyme adsorption. *Bioresour. Technol.* **133** (2013) 270–278.

Ralph, J., Brunow, G., Harris, P.J., Dixon, R.A., Schatz, P.F., Boerjan, W. Lignification: are lignins biosynthesized via simple combinatorial chemistry or via proteinaceous control and template replication? In: *Recent Advances in Polyphenol Research*. F. Daayf and V. Lattanzio (eds.), Wiley-Blackwell, Oxford, Great Britain, 2008, pp. 36–66.

Ralph, J., Lundquist, K., Brunow, G., Lu, F., Kim, H., Schatz, P.F., Marita, J.M., Hatfield, R.D., Ralph, S.A., Christensen, J.H., Boerjan, W. Lignins: Natural polymers from oxidative coupling of 4-hydroxyphenylpropanoids. *Phytochem. Rev.* **3** (2004) 29–60.

Ralph, J., Quideau, S., Grabber, J.H., Hatfield, R.D., Identification and synthesis of new ferulic acid dehydrodimers present in grass cell walls. *J. Chem. Soc. Perkin Trans.* **1** (1994) 3485–3498.

Rolando, C., Monties, B., Lapierre, C. (1992) Thioacidolysis. In: *Methods in Lignin Chemistry*, C.W. Dence, S.Y. Lin (eds.), Springer-Verlag, Berlin, Germany, 1992, pp. 334–349.

Saloheimo, M., Paloheimo, M., Hakola, S., Pere, J., Swanson, B., Nyyssönen, E., Bhatia, A., Ward, M., Penttilä, M. Swollenin, a Trichoderma reesei protein with sequence similarity to the plant expansins, exhibits disruption activity on cellulosic materials. *Eur. J. Biochem.* **269** (2002) 4202–4211.

Sarkanen, K.V., Ludwig, C.H. (eds.) *Lignins: Occurrence, Formation, Structure, and Reactions*. Wiley-Interscience, New York, NY, USA, 1971, 916 p.

Scalbert, A., Monties, B., Lallemand, J.-Y., Guittet, E., Rolando, C. Ether linkage between phenolic acids and lignin fractions from wheat straw. *Phytochemistry* **24** (1985) 1359–1362.

Scheller, H.V., Ulvskov, P. Hemicelluloses. *Annu. Rev. Plant Biol.* **61** (2010) 263–89.

Schmidt, A.S., Thomsen, A.B. Optimization of wet oxidation pretreatment of wheat straw. *Bioresour. Technol.* **64** (1998) 139–151.

Schwarz, W.H. The cellulosome and cellulose degradation by anaerobic bacteria. *Appl. Microbiol. Biotechnol.* **56** (2001) 634–649.

Selig, M.J., Viamajala, S., Decker, S.R., Tucker, M.P., Himmel, M.E., Vinzant, T.B. Deposition of Lignin Droplets Produced During Dilute Acid Pretreatment of Maize Stems Retards Enzymatic Hydrolysis of Cellulose. *Biotechnol. Prog.* **23** (2007) 1333–1339.

Sewalt, V.J.H., Glasser, W.G, Beauchemin, K.A. Lignin impact on fiber degradation. 3. Reversal of inhibition of enzymatic hydrolysis by chemical modification of lignin and by additives. *J. Agric. Food Chem.* **45** (1997) 1823–1828.

Shuai, L., Yang, Q., Zhu, J.Y., Lu, F.C., Weimer, P.J., Ralph, J., Pan, X.J. Comparative study of SPORL and dilute-acid pretreatments of spruce for cellulosic ethanol production. *Bioresour. Technol.* **101** (2010) 3106–3114.

Siqueira, G., Milagres, A.M.F., Carvalho, W., Koch, G., Ferraz, A. Topochemical distribution of lignin and hydroxycinnamic acids in sugar-cane cell walls and its correlation with the enzymatic hydrolysis of polysaccharides. *Biotechnol. Biofuels* (2011) **4**:7.

Sipponen, M.H., Pastinen, O.A., Strengell, R., Hyötyläinen, J.M.I., Heiskanen, I.T., Laakso, S. Increased Water Resistance of CTMP Fibers by Oat (*Avena sativa* L.) Husk Lignin. *Biomacromolecules* **11** (2010) 3511–3518.

Sluiter, J., Ruiz, R.O., Scarlata, C.J., Sluiter, A.D., Templeton, D.W. Compositional analysis of lignocellulosic feedstocks. 1. Review and description of methods. *J. Agric. Food Chem.* **58** (2010) 9043–9053.

Smil, V. Crop residues: agriculture's largest harvest. *BioScience* **49** (1999) 299–308.

Sun, Q., Yang, L. The adsorption of basic dyes from aqueous solution on modified peat-resin particle. *Water Res.* **37** (2003) 1535–1544.

Sun, R.C., Lawther, J.M., Banks, W.B. Extraction and Characterization of Xylose-Rich Pectic Polysaccharide from Wheat Straw. *Int. J. Polym. Anal. Charact.* **4** (1998) 345–356.

Sun, Y., Cheng, J. Hydrolysis of lignocellulosic materials for ethanol production: a review. *Bioresour. Technol.* **83** (2002) 1–11.

Talebnia, F., Karakashev, D., Angelidaki, I. Production of bioethanol from wheat straw: An overview of pretreatment, hydrolysis and fermentation. *Bioresour. Technol.* **101** (2010) 4744–4753.

Thompson, D.N., Chen, H.-C., Grethlein, H.E. Comparison of pretreatment methods on the basis of available surface area. *Bioresour. Technol.* **39** (1992) 155–163.

Turunen, O., Vuorio, M., Fenel, F., Leisola, M. Engineering of multiple arginines into the Ser/Thr surface of *Trichoderma reesei endo*-1,4-β-xylanase II increases the thermotolerance and shifts the pH optimum towards alkaline pH. *Prot. Eng.* **15** (2002) 141–145.

Vainio, U., Maximova, N., Hortling, B., Laine, J., Stenius, P., Simola, L.K., Gravitis, J., Serimaa, R. Morphology of dry lignins and size and shape of dissolved kraft lignin particles by X-ray scattering. *Langmuir* **20** (2004) 9736–9744.

Waterhouse, A.L. Determination of total phenolics. In: *Current Protocols in Food Analytical Chemistry*, R.E. Wrolstad, T.E. Acree, H. An, E.A. Decker, M.H. Penner, D.S. Reid, S.J. Schwartz, C.F. Shoemaker, P. Sporns (eds.), John Wiley & Sons, Inc., New York, NY, USA, 2002, supplement 6, pp. I1.1.1–I1.1.8.

Wayman, M., Lora, J.H. Aspen autohydrolysis. The effect of 2-naphthol and other aromatic compounds. *Tappi* **61** (1978) 55–57.

Wiman, M., Dienes, D., Hansen, M.A.T., van der Meulen, T., Zacchi, G., Lidén, G. Cellulose accessibility determines the rate of enzymatic hydrolysis of steam-pretreated spruce. *Bioresour. Technol.* **126** (2012) 208–215.

Wu, S., Argyropoulos, D.S. An improved method for isolating lignin in high yield and purity. *J. Pulp. Paper Sci.* **29** (2003) 235–240.

Xu, F. Structure, ultrastructure, and chemical composition. In: R.-C. Sun (Ed.), *Cereal Straw as a Resource for Sustainable Biomaterials and Biofuels*, Elsevier, Amsterdam, The Netherlands, 2010, pp. 9–47.

Yelle, D.J., Kaparaju, P., Hunt, C.G., Hirth, K., Kim, H., Ralph, J., Felby, C. Two-dimensional NMR evidence for cleavage of lignin and xylan substituents in wheat straw through hydrothermal pretreatment and enzymatic hydrolysis. *Bioenerg. Res.* **6** (2013) 211–221.

Zhai, H.M., Lee, Z.Z. Ultrastructure and topochemistry of delignification in alkaline pulping of wheat straw. *J. Wood chem. Technol.* **9** (1989) 387–406.

Zhang, D.S., Yang, Q., Zhu, J.Y., Pan, X.J. Sulfite (SPORL) pretreatment of switchgrass for enzymatic saccharification. *Bioresour. Technol.* **129** (2013b) 127–134.

Zhang, Y., Culhaoglu, T., Pollet, B., Melin, C., Denoue, D., Barrière, Y., Baumberger, S., Méchin, V. Impact of lignin structure and cell wall reticulation on maize cell wall degradability. *J. Agric. Food Chem.* **59** (2011) 10129–10135.

Zhang, Y., Legay, S., Méchin, V., Legland, D. Color Quantification of Stained Maize Stem Section Describes Lignin Spatial Distribution within the Whole Stem. *J. Agric. Food Chem.* **61** (2013a) 3186−3192.

Zhao, H., Jones, C.L., Baker, G.A., Xia, S., Olubajo, O., Person, V.N. Regenerating cellulose from ionic liquids for an accelerated enzymatic hydrolysis. *J. Biotechnol.* **139** (2009) 47−54.

Zhao, X., Zhang, L., Liu, D. Biomass recalcitrance. Part I: the chemical compositions and physical structures affecting the enzymatic hydrolysis of lignocellulose. *Biofuels, Bioprod. Bioref.* **6** (2012) 465–482.

Zugenmaier, P. Crystalline cellulose and cellulose derivatives. Characterization and structure. Springer, Berlin, 2008, 285 p.

Lignin is the group of aromatic polymers arising from 4-hydroxyphenylpropanoids. In plants, lignin is an essential structural component protecting cell walls and carbohydrates from enzymatic hydrolysis. Pretreatment is used for overcoming this recalcitrance in a lignocellulosic biorefinery of the biochemical type. This thesis elucidates the structural changes in lignin that occur during various mechanical, chemical and hydrothermal treatments of plant residues. Reduction of the surface area occupied by lignin was elaborated as the preferred way to increase conversion of cellulose to glucose in enzymatic hydrolysis.

Aalto-DD 79/2015

ISBN 978-952-60-6234-1 (printed)
ISBN 978-952-60-6235-8 (pdf)
ISSN-L 1799-4934
ISSN 1799-4934 (printed)
ISSN 1799-4942 (pdf)

Aalto University
School of Chemical Technology
Department of Biotechnology and Chemical Technology
www.aalto.fi